Fall 1996

Effect of lamellar microstructure on the permeability of polyethylene films

Yufu Li
New Jersey Institute of Technology

Copyright Warning & Restrictions

The copyright law of the United States (Title 17, United States Code) governs the making of photocopies or other reproductions of copyrighted material.

Under certain conditions specified in the law, libraries and archives are authorized to furnish a photocopy or other reproduction. One of these specified conditions is that the photocopy or reproduction is not to be "used for any purpose other than private study, scholarship, or research." If a, user makes a request for, or later uses, a photocopy or reproduction for purposes in excess of "fair use" that user may be liable for copyright infringement,

This institution reserves the right to refuse to accept a copying order if, in its judgment, fulfillment of the order would involve violation of copyright law.

Please Note: The author retains the copyright while the New Jersey Institute of Technology reserves the right to distribute this thesis or dissertation

Printing note: If you do not wish to print this page, then select "Pages from: first page # to: last page #" on the print dialog screen

ABSTRACT

EFFECT OF LAMELLAR MICROSTRUCTURE ON THE PERMEABILITY OF POLYETHYLENE FILMS

by
Yufu Li

Lamellar microstructures can decrease the permeability to gases and vapors by increasing the diffusive path in plastic films, or the so-called "tortuosity" which depends on the aspect ratio, orientation, and the volume fraction of the dispersed material. In this research, different types and percentages of mica with relatively high aspect ratio are used as oxygen barrier materials in blown films. Both high and low density polyethylenes (HDPE and LDPE), as well as their blends are used as the matrix materials.

A decrease in permeability of both LDPE and HDPE films to oxygen is achieved with increasing volume fraction of the higher aspect ratio mica. By contrast, use of the coarser mica grades did not result in the anticipated properties in HDPE films. In all cases, the morphology of the films corresponded to several overlapping, discontinuous mica layers with the broad faces of mica, essentially parallel to the surface of the films. Rheological properties, morphology, and mechanical properties were also examined. The experimentally determined permeability and elastic modulus values were found to be in good agreement with theoretical predictions. By contrast to LDPE, the processability of HDPE films was found to decrease dramatically with increasing mica loadings, It was found that optimization of barrier properties in HDPE films through addition of mica flakes is a compromise between the desired reduction in permeability and the loss in processability and ductility.

EFFECT OF LAMELLAR MICROSTRUCTURE ON THE PERMEABILITY OF POLYETHYLENE FILMS

by
Yufu Li

A Thesis
Submitted to the Faculty of
New Jersey Institute of Technology
in Partial Fulfillment of the Requirements for the Degree of
Master of Science in Engineering Science

Interdisciplinary Program in Materials Science and Engineering

October 1996

APPROVAL PAGE

EFFECT OF LAMELLAR MICROSTRUCTURE ON THE PERMEABILITY OF POLYETHYLENE FILMS

Yufu Li

Dr. Marino Xanthos, Thesis Advisor — Date
Associate Professor of Chemical Engineering, Chemistry, and Environmental Science

Dr. Roland A. Levy, Committee Member — Date
Professor of Physics,
Director of Materials Science and Engineering Program

Dr. L. N. Krasnoperov, Committee Member — Date
Associate Professor of Chemical Engineering, Chemistry, and Environmental Science

BIOGRAPHICAL SKETCH

Author: Yufu Li

Degree: Master of Science

Date: October 1996

Undergraduate amd Graduate Education:

- Master of Science in Engineering Science
  New Jersey Institute of Technology, Newark, NJ, 1996

- Bachelor of Science in Materials Science and Engineering
  Beijing University of Aeronautics and Astronautics, Beijing, P. R. China, 1983

Major: Materials Science and Engineering

Presentation:

Yufu Li and Marino Xanthos,
"Effect of Lamellar Microstructure on the Permeability of Plastic Films",
The Sixth Annual Mini-Tech Conference, Stevens Institute of Technology, Hoboken, NJ, April 1996.

To my beloved family

ACKNOWLEDGMENT

I would like to express my deepest appreciation to Dr. Marino Xanthos, my research supervisor, for not only generously providing valuable and countless resources, but also constantly giving me support, encouragement, and reassurance. Special thanks are given to Dr. Roland A. Levy (from whom, my academic advisor, I got all kinds of information and instructions) and Dr. L. N. Krasnoperov for actively participating in my committee.

I am very grateful to Dr. Subir Dey and Dr. Victor Tan of the Polymer Processing Institute (PPI), as well as Mr. Qiang Zhang from NJIT; without their help, this research would not have been successfully completed.

I also wish to thank Mr. Ming-wan Young, Mr. Andy Ponnusamy, Mr. Dale Condi and others from PPI/CPPP for their technical support.

TABLE OF CONTENTS

Chapter	Page
1 INTRODUCTION	1
2 LITERATURE REVIEW	3
2.1 Permeability and Its Measurement	3
2.2 The Physicochemical Nature of the Components and its Effect on Permeability	6
2.3 Previous Work	9
2.3.1 Plastic Laminates	9
2.3.2 Polymer Blends and Polymer-Filler Composites	11
2.3.3 Summary	15
3 EXPERIMENTAL	16
3.1 Selection of Components	16
3.2 Processing	16
3.2.1 Compounding	16
3.2.2 Blown Film Extrusion	19
3.3 Characterization and Testing	23
3.3.1 Rheological Characterization	23
3.3.1.1 Melt Viscosity	23
3.3.1.2 Melt Elasticity Index	23
3.3.2 Morphology	24

TABLE OF CONTENTS
(Continued)

Chapter	Page
3.3.2.1 Transmission Optical Microscope	24
3.3.2.2 Scanning Electron Microscope (SEM)	24
3.3.3 Mechanical Properties	24
3.3.4 Oxygen Permeability	26
4 RESULTS AND DISCUSSION	30
4.1 Materials	30
4.1.1 Selection of Components	30
4.1.2 Compounding	30
4.2 Materials Characterization	31
4.1.1 Apparent Shear Viscosity	31
4.1.2 Melt Elasticity Index	38
4.3 Blown Film Extrusion	40
4.4 Morphology of Blown Films	42
4.4.1 Transmission Optical Microscope Study	42
4.4.2 Scanning Electron Microscope Analysis	46
4.5 Mechanical Properties of Blown Films	51
4.5.1 Tensile Stress	52
4.5.2 Elastic Modulus	57
4.5.3 Elongation at Break	60

TABLE OF CONTENTS
(Continued)

Chapter	Page
4.6 Permeability to Oxygen	60
4.6.1 Considerations for the Experiment	60
4.6.2 The Effects of Materials Structure	62
5 CONCLUSIONS AND RECOMMENDATIONS	71
REFERENCES	73

LIST OF TABLES

Table		Page
3.1	Principal properties of polyethylene resins	17
3.2	Principal properties of micas	18
3.3	List of compositions	20
3.4	Processing conditions of blown films	22
4.1	Shear viscosities of PE and PE/Mica composites (pellets and films)	37
4.2	Melt elasticity indices of PE and PE/Mica composites blown films	39
4.3	Dimensions and distribution of mica flakes in blown films	45
4.4	Mechanical properties of blown films in the machine direction	53
4.5	Mechanical properties of blown films in the transverse direction	54
4.6	Permeability of blown films to oxygen	63

LIST OF FIGURES

Figure — Page

3.1 Schematic sketch of blown film extrusion line 21

3.2 Schematic sketch of melt elasticity indexer 25

3.3 Experimental set-up for permeability test 27

3.4 Typical plot of oxygen volume change as a function of time (HDPE film, thickness=0.0368 mm, pressure difference=103.43 mmHg) 28

4.1 Effect of different micas (10 wt%) on the viscosity of HDPE at 230°C 32

4.2 Effect of Mica325HK on the viscosity of LDPE at 190°C 33

4.3 Effect of Mica325HK on the viscosity of HDPE at 230°C 34

4.4 Effect of Mica200HK on the viscosity of HDPE at 230°C 35

4.5 Effect of Mica200PE on the viscosity of HDPE at 230°C 36

4.6 TOM micrograph showing morphology of the surface of HDPE/ 5 wt% Mica325HK composite blown film (400 X) 43

4.7 TOM micrographs showing morphology of the surfaces of HDPE/mica composites blown films 44

4.8 SEM micrograph showing morphology of the cross-section of HDPE/5 wt% Mica325HK composite blown film 47

4.9 SEM micrographs showing morphology of the cross-section of HDPE/mica composites blown films 48

4.10 Schematic sketch of mica dimensions and distribution in blown film 50

4.11 Stress at break as a function of polyethylene/mica composition and mica weight percentage 55

4.12 Yield stress as a function of polyethylene/mica composition and mica weight percentage 56

LIST OF FIGURES
(Continued)

Figure | Page

4.13 Young's modulus as a function of polyethylene/mica composition and mica weight percentage 58

4.14 Strain at break as a function of polyethylene/mica composition and mica weight percentage 61

4.15 Oxygen permeability of three polyethylene films with different densities as indicated in the brackets 64

4.16 Effect of mica on the oxygen permeability of LDPE films 67

4.17 Effect of Mica325HK on the oxygen permeability of HDPE films 68

4.18 Comparison of measured and calculated oxygen permeability for the polyethylene/mica films 69

4.19 Effect of Mica200HK and Mica200PE on the oxygen permeability of HDPE films 70

CHAPTER 1

INTRODUCTION

In recent years, there has been a rapid increase in the number and variety of challenges and opportunities facing scientists and engineers in the areas of permeability-controlled materials and processes. Conventional techniques are insufficiently flexible or too costly in many cases, and advanced processes are being developed to meet new needs.

The permeation behavior of low molecular weight substances in polymeric materials is a topic of interest for many fields of science and technology. Two aspects of the permeability-controlled applications of thin polymeric materials, such as films and membranes, are the most interesting. One of the fields is separation membrane systems, including reverse osmosis, ultrafiltration, and bioprocess applications, etc.. The other field includes highly impermeable or selectively permeable packaging or barrier films for applications such as organic fluid containers, and oxidation and humidity resistant packaging. The latter type of application is our consideration in this research.

A plastic material which has low permeability to one permeant may have high permeability to another permeant. Various combinations of materials and processes for improving permeation properties emerge logically. In industrial practice and laboratory research, the most general designs for reducing permeability are continuous lamellar structures, including laminated composites, plastic coatings and coextruded multilayer structures. For example, HDPE (high density polyethylene) is a barrier for water, but not oxygen; on the other hand, PA (polyamide) has excellent low oxygen permeability but is

sensitive to water. HDPE/PA multilayer composite structures can remarkably reduce the permeability of both water and oxygen. Lamellar microstructures in polymer blends and inorganic filler composites can also be made by carefully designing the manufacturing processes. These products may be characterized by lower cost and easier recycling as compared to continuous laminated structures.

The term "barrier plastics" is applied to several groups of plastics which have very low permeability to gases and/or water vapor. Different techniques have been developed to produce such materials. These techniques are: (a) layering of polymers with different barrier properties by coextrusion, lamination or coating, as well as metallizing; (b) molecular orientation, such as biaxial stretching; (c) blending with other polymers; and (d) addition of solids, such as mica, talc or aluminum flakes. The latter method is studied in this research.

Polyolefins have outstanding barrier properties to water, but their high permeability to many organic solvents and gases limits their use in certain industrial and packaging applications. By combining polyolefins with platy fillers, discontinuous lamellar structures are produced. The increase of the diffusion path (tortuosity) in the polymer/platy filler film, results in the decrease in permeability.

The main objective of this research was to study the effect of lamellar microstructure obtained through flow orientation on the permeability of oxygen through polyethylene/ mica films. The processability of polyethylene containing different grades of mica was analyzed, as well as the melt viscosity and elasticity characteristics of the mixture. The mechanical properties of the extrusion blown films were also tested.

CHAPTER 2

LITERATURE REVIEW

2.1 Permeability and its Measurement

The transport of matter through a slab or film, in the absence of cracks, pores, or other gross defects, is usually considered to occur by the sequential process: solution (condensation, then mixing) of the gas or liquid in the upstream surface, migration through the bulk material by activated diffusion to the opposite (downstream) surface, and desorption from the downstream surface into a gaseous or liquid phase. This process is named permeation. The capability of permeation of a material is the "permeability".

In the permeation of non-condensible gases in polymeric films, equilibrium levels of gas sorption in the solid are low because interaction between solute molecules and the polymer are weak. The equilibrium concentration(C) of gas absorbed in the polymer can be related to the partial pressure(p) of the gas by Henry's law [1]:

$$C=S.p \tag{2.1}$$

where S is the solubility coefficient.

The flux, J, of a substance in the film is defined as the amount passing during unit time through a surface of unit area normal to the direction of flow. The diffusivity D is defined in Fick's first law [2]:

$$J=-D(\frac{\partial C}{\partial X}) \tag{2.2}$$

The diffusion coefficient D is independent of the concentration C. The length X is the distance between any two points on the flow vector.

For simple gases, the permeability P is the product of the diffusivity D and the Henry's law solubility constant S [3]:

$$P=D.S \tag{2.3}$$

It has been found [2] that the permeability varies with temperature according to a Van't Hoff-Arrhenius Equation:

$$P=P_0\exp(-\frac{E_p}{RT}) \tag{2.4}$$

where E_p is the apparent activation energy for the permeation process, R is the gas constant, and T is the temperature.

Many techniques have been used to measure the transmission rate of low-molecule-weight penetrants through a polymer membrane. Experimental methods, apparatus and calculation for the determination of S, D and P have been well discussed by Felder and Huvard [4]. There are several ASTM standard methods established for testing gas permeability through plastic films and sheets [5], [6].

If a film of thickness *l* and area A separates two chambers containing a permeable gas at different pressure, then the gas will permeate from the high pressure chamber to the low pressure chamber. The plot of Q (the amount of gas to permeate the film) versus time t shows an initial build up period but eventually a linear relationship develops as t $\rightarrow\infty$. At this condition, the simplified relation between Q and t is [7]:

$$Q=\frac{DC_1}{l}(t-\frac{l^2}{6D}) \tag{2.5}$$

where C_1 is the concentration of gas in the face of the film adjacent to high pressure chamber. The interception on the time-axis is known as the time lag θ [7], which is:

$$\theta=\frac{l^2}{6D} \tag{2.6}$$

This equation provides the basis for the determination of D by the time lag method. If we know S, then P is very easy to estimate using Equation 2.3.

If the gas pressures are now p_1 and p_2, then the concentrations at the film surfaces are C_1 and C_2. The flux is given by Fick's first law (Equation 2.2) [2], i.e., in the steady state:

$$J=-D\frac{(C_2-C_1)}{l} \tag{2.7}$$

The total amount of permeant passing through a film of area A after time t is:

$$Q=-DAt(C_2-C_1)/l \tag{2.8}$$

It is assumed that Henry's law (Equation 2.1) applies at both interfaces [7], i.e.,

$$S=\frac{C_1}{p_1}=\frac{C_2}{p_2} \tag{2.9}$$

Hence, Equation 2.8 can be written as

$$Q=-DSAt(p_2-p_1)/l \tag{2.10}$$

For a simple gas (Equation 2.3) [3]:

$$P=DS=\frac{Ql}{At(p_1-p_2)} \tag{2.11}$$

Experimental conditions can be arranged for $p_1 \gg p_2$, therefore, Equation 2.11 can be simplified as:

$$P=\frac{Ql}{Atp_1} \tag{2.12}$$

The SI unit of the permeability coefficient is [5]: mol/(m.s.Pa). Usually the unit of "Barrer" is used, it stands for: 10^{-10}ml (STP)/(cm.s.cmHg). Equation 2.12 is normally employed for the experimental determination of permeability.

2.2 The Physicochemical Nature of the Components and Its Effect on Permeability

In order to understand the mechanisms of transport in the various plastics, it is useful to consider features of the two principal microstructural conditions of plastic materials: the glassy and rubbery states. In the glassy state, the mobility of polymer chain is restricted due to the limitation of rotation about the chain axis. By contrast, polymers in the rubbery state typically are associated with higher chain mobility. In this case, long segments participate in the diffusion process due to internal micromotion of chain rotation and transition, which form larger amounts of free volume and transit these spaces easier. In terms of the free volume theory [7], any factor which tends to render polymer chain segments less mobile or to pack more closely will decrease the diffusion and permeation

rates. The density of polymer, as related to the free-volume, is a measure of the "looseness" of the polymer structure.

In both glassy and rubbery states, the gas transport characteristics can be further modified by the presence of a crystalline phase, or by stress-induced orientation. The crystalline phase in a polymer has at least two effects on sorption and diffusion behavior. At temperatures well below the melting point, crystalline regions are generally inaccessible to most penetrants. Hence, they act as excluded volumes for the sorption process and as impermeable barriers for the diffusion process. A tortuosity factor, τ, is proportional to the crystalline volume fraction. The other effect, β (a "cross-linking" effect), is that crystalline domains act as giant crosslinking regions with respect to those chains which enter and leave those regions from the surrounding non-crystalline matrix in which sorption and diffusion take place, so the effect of crystallinity on the diffusion constant is expressed [7] as:

$$\tau\beta = D^*/D \tag{2.13}$$

where D^* is the diffusion constant in completely amorphous polymer and D is the diffusion constant of the polymer with crystalline regions at the same temperature. For amorphous homopolymers, drawing can, under certain circumstance, bring about decreases in the rate of transport in the direction normal to the draw axis, and substantial changes in permeability occur when crystallizable polymers are stretched, owing in part, to changes in the shape, extent and perfection of the essentially non-permeable crystalline regions.This is elucidated by Heffelfinger [8].

Besides the morphology of the polymer and many physical factors, the chemical structure of a polymer is considered to be the predominant factor which controls the magnitude of the permeability. The solubility of permeant gases in polymers at normal temperatures is very low, usually less than 0.2% [1]. As a general rule, the well-known principle of "like dissolves like" is applicable. The presence of impurities, such as catalyst fragments or additives, within a polymer may seriously affect the solubility process.

The magnitude of the solubility is dependent on the size and shape of the penetrant molecule. Diffusion generally decreases as the molecular size increases. As a consequence of this nearly compensating dependence of D and S on penetrant size and shape, the permeability, P=D.S, is much less dependent on the size and shape of the penetrant than is either D or S individually.

Setting other factors equal, the permeation rate of gases can be expected to decrease as the structural symmetry and cohesive energy of the polymer increase. On the basis of an investigation of the effects of short-chain branching on the moisture permeability of vinyl-type polymers, Lasoski [9] concluded that an unsymmetrical substitution of pendent groups on the main chain leads to an increased permeability. In a comparison of two symmetrical polymers, such as polyvinylidene chloride (PVDC) and polybutadiene (BR), the former is found to be more polar, which leads to a much lower diffusion coefficient to oxygen due to its high cohesive energy. Chemical modification of a polymer can have a pronounced effect on P and D. The introduction of methyl or polar side groups onto rubber chains increases the cohesive energy and decreases the values of P and D, but only slightly affects the S. The presence of double bonds in main polymer chains tends to increase the D.

2.3 Previous Work

2.3.1 Plastic Laminates

Physicochemical properties and varying polymerization processes affect the permeability of the plastic films. There is no single film which meets all of the requirements for the desired properties. However, with plastic laminates, the required properties can be achieved.

The permeation through multilayer plastic laminates comprised of two or more materials or phases can be complex, depending on the nature and magnitude of component interactions, the amount and distribution of the multi-phases, interphase mixing regions and any interfacial phenomena. In the simplified case, it is assumed that the rate of transport is the same across each layer so that permeability is not a function of pressure or concentration, and that there are no barriers to diffusion due to interfacial phenomena; then, the permeability of n layers with the total thickness l is given by the harmonic average of the weighed individual permeability P_i of i th layer of thickness x_i [2]:

$$\frac{1}{P} = \sum_{i=1}^{n} \left(\frac{x_i}{l}\right)\left(\frac{1}{P_i}\right) \qquad (2.14)$$

It is obviously shown that any one layer with low permeability to a penetrant can significantly lower the permeability of the plastic laminate to the penetrant. Theoretically, if each layer in a plastic laminate applies a specific low permeability, the plastic laminate will have low permeability to all penetrants.

The so-called "barrier materials" are relative to certain penetrants. Generally speaking, polar materials are more or less hygroscopic, but with excellent non-polar gas

impermeability and vice versa. We usually place these hygroscopic materials as inside layers due to their decreasing barrier properties in humidity environment. It is also important to prevent barriers from crashes and other damage.

A typical plastic laminate includes different materials based on their functions. Barrier materials to reduce permeability, structural materials to achieve certain mechanical properties, and adhesive materials to hold the plastic laminate together.

The structural plastic is usually a polyolefin. Polyolefins are generally good moisture barriers and have additional function of protecting the barrier layers from moisture. The choice of materials for the structural layers depends on the product requirements and may be different on either side of the product. Barrier layers are selected materials, such as PA, EVOH (Ethylene-vinyl alcohol copolymer), PET (Polyethylene terephthalate), PVDC, with excellent gas/hydrocarbon impermeability. Very thin layers can achieve the permeation requirement in packaging. Perdikoulias and Wybenga [10] considered that a uniform EVOH layer with thickness of 0.4 μm is somewhat impractical. A more realistic value is a layer thickness of 8 - 10 μm. Hensen [11] recommended a thickness of 5 μm for the EVOH layer in coextrusion. Layer continuity is retained by a critical lamella thickness which can inhibit layer breakup [12]. Different techniques are used for the measurement and control of thickness of the barrier layers [13]. In cases in which the structural and barrier materials are not compatible, a very thin tie layer is employed for good adhesion between the two layers. For example, EVA (Ethylene vinyl acetate) can be used to bond PVDC to PP, and EMAA (Ethylene methacrylic acid) (with a low-weight percent of MAA comonomer) can be used to bond ionomer to LDPE (Low density polyethylene). Tanny [14] studied many different bonding agents for coextrusion process.

The tie layer is of practical importance to the end use for both permeability and mechanical properties.

The multilayer plastic product can be made by several industrial plastic processing techniques, such as coextrusion, injection molding, blown film etc.. Coextrusion provides multiple molten layers - usually uses more than one extruder with melts going through one die - that are bonded together. The key technique is the layer formation and combination. Basically the feed-block, multiple manifold or combination of these two are used [15]. Blown film line can also produce multilayer products, mainly packaging materials, by the same working principle of the coextrusion. Lamellar injection molding combines coextrusion and injection molding technology to enable the molder to create a micron scale layered morphology in complex asymmetric multicavity parts [12]. Barrier film coatings add performance options [16].

2.3.2 Polymer Blends and Polymer-Filler Composites

A polymer blend used for barrier purposes usually comprises a more permeable polymer as matrix and a low permeability polymer dispersed in the matrix phase with or without the addition of interfacial agent. If an inorganic filler substitutes the low permeability polymer as barrier, the blend becomes a polymer-filler composite. These multiphase materials can decrease permeability by increasing the diffusion path, the so-called "tortuosity effect" [17]. The tortuosity effect depends primarily on two factors: barrier material volume fraction, and its aspect ratio. Aspect ratio can be defined as the ratio of length over diameter for fibers, or the ratio of equivalent diameter or largest dimension on an X-Y plane over thickness. A dispersed phase with a large aspect ratio ribbons or

platelets can significantly decrease permeability through the formation of a discontinuous lamellar structure in which the broad faces of platelets are normal to the flow direction of permeant. Yeh et. al. [18] examined the effects of aspect ratio and concentration on the relative effective diffusivity of HDPE/PA-6 blends theoretically, and indicated that there is a critical aspect ratio between 50 and 75, and a critical concentration between 10% and 12%. At the region of low aspect ratios, the effective diffusivity shows an approximately linear decrease proportional to the concentration of the nylon. At the region of high aspect ratios, a critical concentration is found and the effective diffusivity slightly decreases above the critical concentration.

The lamellar morphology of polymer blends is determined by shear rate, interfacial tension, initial domain size, composition, flow field, viscosity and melt elasticity of the components. In most case, barrier products are produced by extruder, so that the reported observations and researches are mostly related to the process of extrusion.

Kamal et al [19] analyzed the effect of various parameters on PP/EVOH, MAPP/EVOH, PE/PA6 based blends, and observed that a metering screw works better than a mixing screw to form lamellar structures; thus, lower shear force and less mixing are preferred. Another important material characteristic which affects the morphologies of blends is the viscosity of the components. The high melt temperature and high viscosity of the matrix, both of which result in viscosity ratio (η_M/η_d) close to 1, are more desirable to produce lamellar morphology in HDPE/PA6 blends [20], [21]. On the other hand, in PP/EVOH blends the viscosity of EVOH is always higher than that of PP over broad ranges of temperature and shear rate [20]. Miura et al [22] preferred Nylon with a higher viscosity than HDPE in promoting lamellar structure, so that the matrix envelops

the dispersed phase during processing. Either very high or very low viscosity ratio does not help the formation of lamellar morphology. Kamal et al [19] gave some examples of the relation of dispersed phase morphology versus viscosity ratio.

It is well established that extensional flow is more efficient than shear flow in deformation of the dispersed phase [23]. Following this principle, Kamal and co-workers [20] achieved lamellar morphology under controlled processing conditions using a special die design incorporating converging and diverging sections. Subramanian [24], [25] was able to develop lamellar morphology for blow molded containers using PE/PET and PE/PA6 blends. Xanthos et al [26] investigated flow induced evolution of lamellar structure upon injection molding of polyolefins blends. Under various conditions in PP/PA/compatibilizer system, spherical morphology of dispersed phase was preserved even after injection molding due to the high maleic anhydride content of the compatibilizer. The PP/PA blends, extruded with a lower functionality compatibilizer, depicted a coarser dispersed structure, which eventually stretched to a lamellar shape in injection molding. Kamal et al [21] studied PE/PA systems with different degree of compatibilization. It appears that exceeding an optimum value of compatibilization by decreasing the interfacial tension below a certain value, tends to erode the lamellar morphology. The determination of optimum compatibilizer level is currently under investigation. Compatibilization needs to offer a compromise between deformation and encapsulation, and good adhesion between the components; also, between permeability and mechanical properties.

The effects of composition of polymer blends on the permeability were investigated by Subramanian [25] who also studied the HDPE/PA6 system. He concluded that modest

to good permeability barrier properties to hydrocarbons are obtained at concentrations of 5 to 10 percent PA6, and the optimum barrier properties are obtained at 18 percent PA6. Lohfink and Kamal [19] showed that the batch mixed PP/EVOH blends decreased the permeability to oxygen as the volume percentage of EVOH increased. The lamellar extrusion blends, with more than 24% EVOH (by volume) in PP or MAPP matrix, showed oxygen permeation results similar to those of coextrusion composites. Minimum fraction of barrier material, including both polymeric and inorganic fillers, is necessary for achieving overlapped morphology in the plastic barrier products.

Inorganic fillers in polymer-filler composites usually function as reinforcements and often serve for reducing cost. Platelet-shaped fillers such as talc, mica, and aluminum flakes, with large aspect ratio have been shown to improve the barrier properties of the composites through the tortuosity effect. Murthy et al [27] used PE and PA as matrix materials with loadings of 20 and 60 phr talc (1.5-14 μm size), and analyzed the effect of the platelet shaped talc on oxygen and water vapor transmission rate through thin PE and Nylon film blow-molded in 38 μm and 51 μm respectively. In both PE and Nylon 6 films, the platelet shape of the talc flakes was oriented parallel to the plane of the film resulting in higher barrier exposed area and increased tortuosity. The rate of water vapor transmission through PE film can be decreased by as much as 50%. The oxygen permeability as well as water vapor transmission rates are similarly reduced by the talc in the Nylon 6 film. Further improvement in the desired orientation is achieved when there is biaxial stretching of the melt following extrusion such as that occurring during blown film production. The barrier properties change with the size of the filler, the smaller size being more favorable. This may be due to the fact that the maximum aspect

ratio can only be achieved in very fine particle size [28]. Bissot [29] concluded that there are basically three types of platelet type fillers that can be considered for thin film structures. These are aluminum flake, mica, and talc. Others are either too large in particle size or else have too low an aspect ratio to be useful. Gill and Xanthos [30] investigated the effect of the morphology and concentration of talc on the permeability of HDPE blown films to oxygen, and found a significant decrease in permeability as the talc loading increases with a concomitant reduction in processability.

2.3.3 Summary

Lamellar structures containing barrier materials, either on a macroscopic level such as continuous plastic laminates or on a microscopic level such as overlapped and oriented discontinuous ribbons and platelets, dispersed in the polymer matrix, can be very effective in reducing permeability of plastic products to gases, hydrocarbons or water. For the continuous structures the forming barrier depends on the nature of materials and the thickness of the barrier layer. For the latter, besides the nature of materials, one also needs to carefully control the processing parameters in order to form and orient the overlapping ribbons or platelet-shaped barrier.

CHAPTER 3

EXPERIMENTAL

3.1 Selection of Components

The primary resin used in this research is high density polyethylene (HDPE Paxon AD06-007). Low density polyethylene (LDPE Dow 640 I) was also used as the reference material. The phlogopite type mica (an aluminum-potassium orthosilicate $[K_2(MgFe^{+2})_6(Al_2Si_6O_{20})(OH, F)_4]$) [31] is supplied by Suzorite Mica Products Inc. The principal properties of polyethylenes from Reference 32 are listed in Table 3.1, and the properties of mica from both manufacturer and Reference 31 are listed in Table 3.2, respectively.

3.2 Processing

3.2.1 Compounding

The following composites were compounded using a twin screw extruder: (a) LDPE/Mica325-HK (90 wt%/10 wt%); (b) HDPE/Mica325-HK (90 wt%/10 wt%); (c) HDPE/Mica200-HK (90 wt%/10 wt%); and (d) HDPE/Mica200-PE (90 wt%/10 wt%). Twin screw compounding were carried out on a 30 mm co-rotating intermeshing twin-screw extruder (ZSK 30, Werner and Pfleiderer) with a L/D ratio of 42:1. The operating temperatures are 230°C (HDPE) and 190°C (LDPE). Mica was added downstream into the polyethylene melt. The mixture was extruded through a 6 mm diameter strand die, into a water bath, and pelletized.

Table 3.1 Principal Properties of Polyethylene Resins

	HDPE	LDPE
Commercial name	Paxon AD60-007	LDPE 640 I
Manufacturer	Paxon	Dow Chemical
Grade	Blown Molding	Blown Film
Melt Flow (g/10 min)	0.70 (190/2.16)	2.0 (190/2.16)
Density (g/cm^3)	0.96	0.922
Tensile stress, Yield (MPa)	30	11
Tensile Modulus (MPa)	1068	-
Elongation, Break	600%	600%

Table 3.2 Principal Properties of Micas

	Mica 325-HK	Mica 200-HK	Mica 200-PE
Color	Golden brown	Golden brown	Golden brown
Shape	Thin flakes	Thin flakes	Thin flakes
Average size (μm)	21	45	45
Specific gravity (g/cm^3)	2.9	2.9	2.9
Tensile strength* (MPa)	255 - 296	255 - 296	255 - 296
Tensile modulus* (GPa)	172	172	172
Thermal conductivity* (cal/cm^2/sec/cm/°C)	16×10^{-4}	16×10^{-4}	16×10^{-4}
Surface treatment	No	No	Yes

* Data from Reference 31

Some of the compounds of HDPE with various micas are then diluted with neat resins to produce compositions with 7.5% and 5% by weight of mica. The various compositions used in this work are listed in Table 3.3.

3.2.2 Blown Film Extrusion

Film blowing is the most important method for producing polyethylene films. This process offers optimum efficiency and other advantages, like variability in the width and thickness dimensions, and the outstanding mechanical properties obtained by biaxial orientation. In this research, all compositions (see Table 3.3) were run on the blown film extrusion line. The Sterling blown film extruder has a single flighted screw of 3.81 cm (1.5 inch) in diameter and a L/D ratio of 24. The plastic melt was extruded through a 10.16 cm O.D. (4.0 inches) annular die with a die gap of 0.762 cm (30 mils). The schematic drawing of the Sterling blown film line is shown in Figure 3.1. The thickness of the films was controlled depending on the processability of the compounds. Processing conditions are listed in Table 3.4. The blow-up ratio (BUR) is calculated based on the diameters of the bubble and the die:

$$\text{blow-up ratio} = \frac{\text{bubble diameter}}{\text{die diameter}}$$

The draw ratio can be defined as:

$$\text{draw ratio} = \frac{\text{die gap}}{\text{thickness} \times \text{blow-up ratio}}$$

Table 3.3 List of Compositions

Plastic Matrix	Fillers	Matrix/Filler Ratio by Wt.
HDPE AD60-007	None	100/0
HDPE AD60-007	MICA325HK	95/5, 92.5/7.5, 90/10
HDPE AD60-007	MICA200HK	95/5, 92.5/7.5, 90/10
HDPE AD60-007	MICA200PE	95/5, 92.5/7.5, 90/10
LDPE 640I	None	100/0
LDPE 640I	MICA325HK	90/10
HDPE/LDPE (1:1)	None	100/0
HDPE/LDPE (1:1)	MICA325HK	90/10

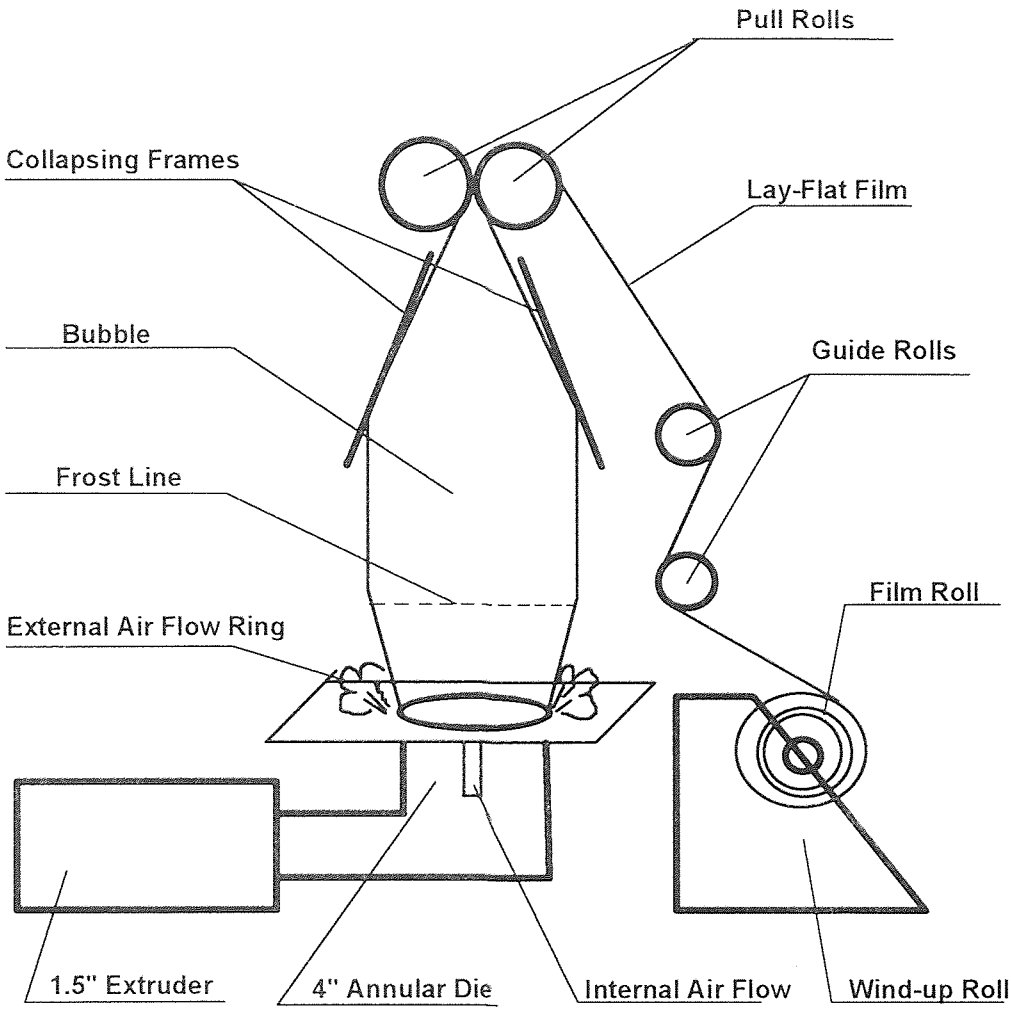

Figure 3.1 Schematic sketch of blown film extrusion line

Table 3.4 Processing Conditions of Blown Films

Materials	Temp. Profile*	V_{screw} (rpm)	V_{nip} (m/min)	Air Vol. (gauge)	Thickness (mm)	Blow-up ratio	Draw ratio
LDPE	A	20	3.05	2.8	0.053	1.48	9.7
LDPE/M325HK (10 wt%)	A	20	3.05	2.8	0.070	1.48	7.3
HDPE	B	40	6.10	2.5	0.044	1.67	10.3
HDPE/M325HK (5 wt%)	B	30	4.57	2.5	0.088	1.51	5.7
HDPE/M325HK (7.5 wt%)	C	25	2.13	2.0	0.136	1.23	4.6
HDPE/M200HK (5 wt%)	B	36	3.96	2.5	0.113	1.63	4.1
HDPE/M200HK (7.5 wt%)	C	25	2.13	2.0	0.189	1.19	3.4
HDPE/M200PE (5 wt%)	B	30	4.57	2.5	0.089	1.67	5.1
HDPE/M200PE (7.5 wt%)	C	25	2.13	2.0	0.166	1.19	3.9
HD/LDPE (1:1)	C	25	3.05	2.0	0.063	1.36	8.9
(HD/LD)/M325HK (10 wt%)	C	25	3.05	2.0	0.170	1.43	3.1

* Temperature settings from hopper to die:
A: 190, 205, 205, 205, 205°C;
B: 190, 230, 230, 240, 240°C;
C: 190, 220, 220, 230, 230°C.

3.3 Characterization and Testing

3.3.1 Rheological Characterization

3.3.1.1 Melt Viscosity: The shear viscosity of the polyethylene resins and the corresponding compounds in pellet form was measured using an automatic capillary rheometer (Monsanto 66-1). The experiments were conducted at temperatures of 190°C and 230°C for the LDPE and HDPE resins and compounds respectively. The diameter, 2r, of the capillary is 1.041 mm, and the ratio L/D is 15. The diameter, 2R, of the barrel is 9.550 mm, and the volume, V, of the extrudate is 1179.89 mm^3. The gage force values of 89, 133, 178, and 222 N (20, 30, 40, and 50 pounds) are used to obtain the shear rate ranging roughly from 100 s^{-1} to 1000 s^{-1}. The initial dwelling time is 5 min. The shear rate is calculated using the following equation:

$$\dot{\gamma} = \frac{4V}{\pi r^3 t} \qquad (3.1)$$

The apparent shear viscosity is calculated by:

$$\eta_a = \frac{tFr^4}{8R^2LV} \qquad (3.2)$$

where t is the time of extrusion process, and the force imposed on the testing material is F which is the product of gage force by 5 as given by the manufacture of the equipment.

The shear viscosity of the materials after being processed into films was also measured.

3.3.1.2 Melt Elasticity Index: The melt elasticity indices (MEI) of the materials after being processed into films were measured using a Melt Elasticity Indexer (Custom Scien-

tific Instruments, Cedar Knoll, NJ) sketched in Figure 3.2. The semiannular specimens with thickness of 2.29 mm (90 mil) were prepared by compression molding. Testing conditions were temperature of 190°C, preheat time of 6 minutes, strain rate of 4 strain units per second, and total strain of 11 strain units (one revolution). Recoverable strain (an indication of melt elasticity) was measured as a function of time. Details on the experimental procedures can be found in Reference 34.

3.3.2 Morphology

3.3.2.1 Transmission Optical Microscope: Blown film samples were examined in the transmission mode of the Zeiss Optical Microscope at 400X and 250X magnifications. The sample was placed on top of the glass platform and a polarized high intensity light was transmitted through it.

3.3.2.2 Scanning Electron Microscope (SEM): Small specimens were randomly cut from the blown films, then embedded in an epoxy resin and cured at 70°C. These specimens were soaked in liquid nitrogen until rigid, then broken quickly to get clean cross-section fracture surfaces. These specimens were sputter-coated with gold-palladium and viewed under SEM. Micrographs of the specimens in typical regions were taken at several magnifications.

3.3.3 Mechanical Properties

A Universal Tinius-Olsen Tester was used for tensile testing. Film samples of 152.4 × 12.7 mm (6" × 0.5") for the modulus test and 101.6 × 12.7 mm (4" × 0.5") for strength

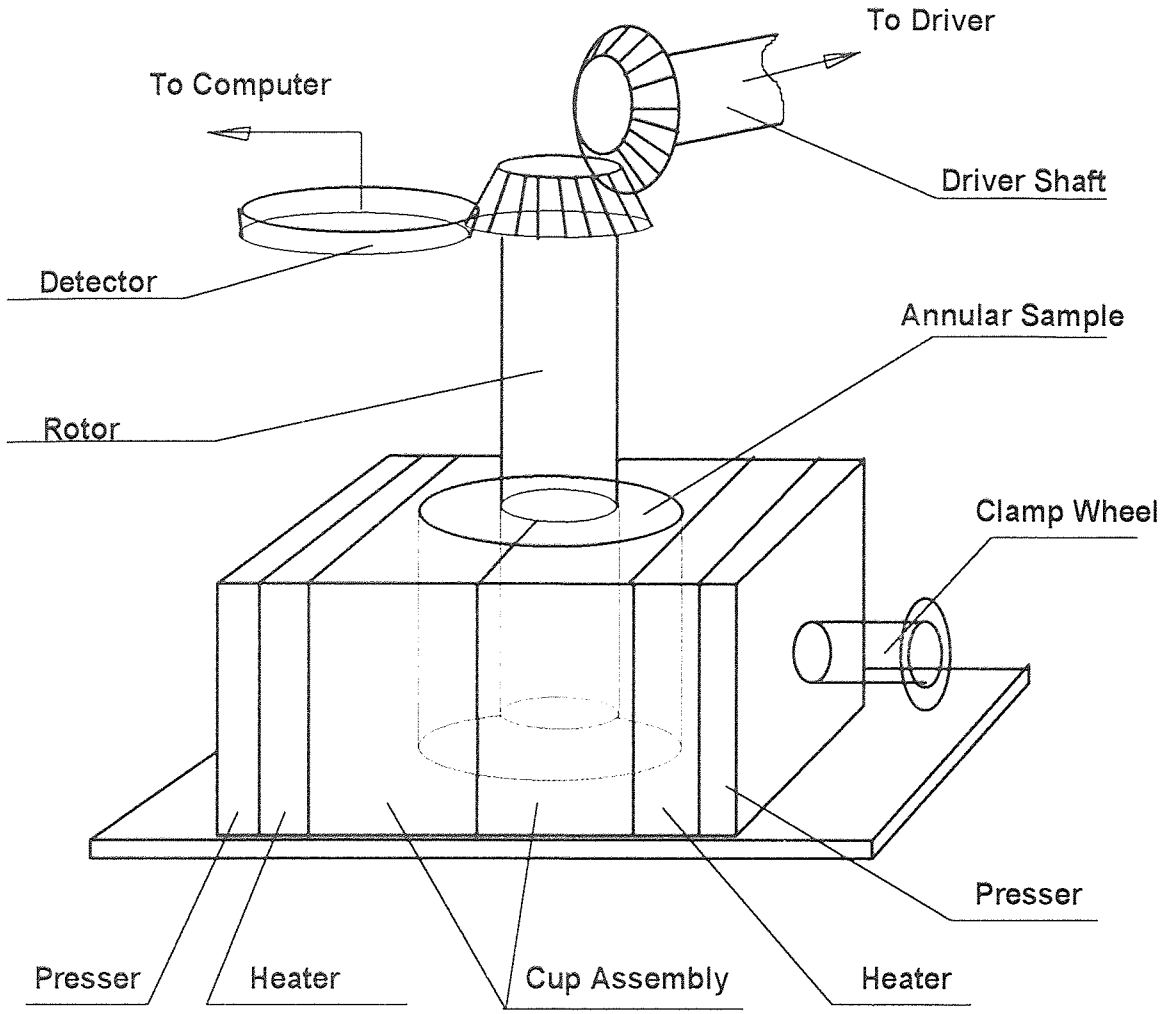

Figure 3.2 Schematic sketch of melt elasticity indexer

and elongation tests were cut in the machine and transverse directions at random locations. A clean cut is essential to prevent nicks and tears, which are likely to cause premature failure. The initial grip separation was 101.6 mm for the modulus test, and 50.8 mm for the other tensile property tests. Cross-head speeds as per ASTM D882 were: a) 10 mm/min for Young's modulus; b) 508 mm/min for LDPE tensile stress-strain; and c) 25.4 mm/min for HDPE (including HDPE/LDPE) tensile stress-strain. A pair of air-actuated grips was employed for better clamping.

3.3.4 Oxygen Permeability

Oxygen permeability of the films was measured according to procedure V in ASTM D1434-82. The experimental set up for the permeation test is shown in Figure 3.3. The test area has a diameter of 44.41 mm. Bone dry oxygen gas was used as permeant, and distilled water as capillary liquid. Specimens were selected at random regions of blown films. The thickness of film was measured at five points within the test area, and then averaged. The experiment was conducted at 23 ± 2°C. The volume, V, of oxygen gas transmitted through the specimen and the corresponding times was recorded after attaining steady-state overnight. The standardized oxygen volume is plotted versus time as shown in Figure 3.4. The slope dV/dt is obtained by linear regression of the plot. The permeability, P, is calculated using the following equation:

$$P = \frac{dV}{dt} \cdot \frac{l}{A\ \Delta p} \qquad (3.3)$$

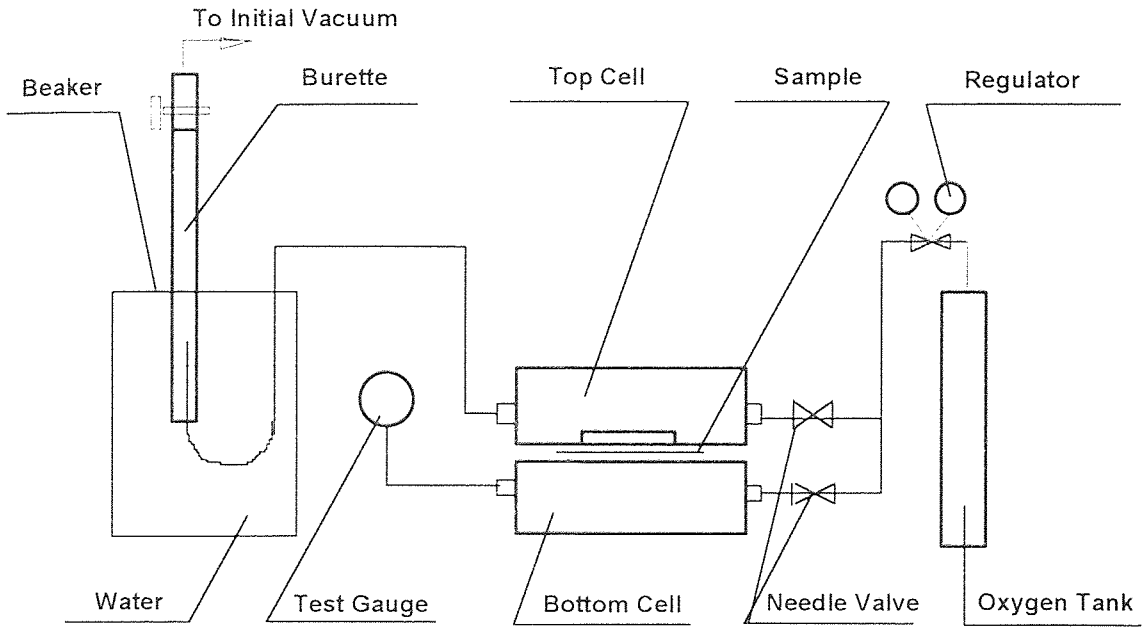

Figure 3.3 Experimental set-up for permeability test

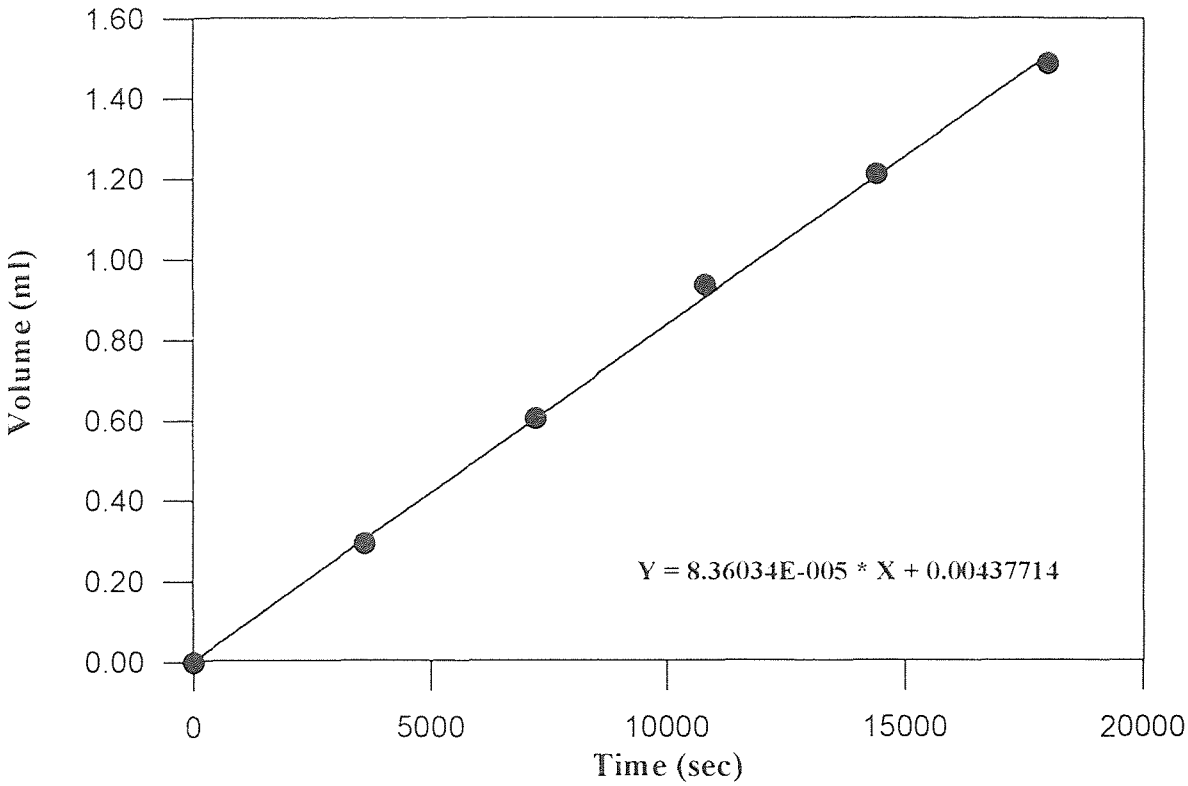

Figure 3.4 Typical plot of oxygen volume change as a function of time (HDPE film, thickness = 0.0368 mm, pressure difference = 103.43 cmHg)

where l and A are the thickness and the area of the test specimen respectively, Δp is the pressure difference between the two sides of the specimen.

CHAPTER 4

RESULTS AND DISCUSSION

4.1 Materials

4.1.1 Selection of Components

Various grades of polyethylene are extensively used in the packaging industry due to their excellent processability, good mechanical properties, low cost, and safety for food applications. However, the permeability of polyethylene to oxygen is not satisfactory. Different techniques can be used to reduce the permeability of plastics to gases or vapors. In this research, the FDA approved HDPE, Paxon AD60-007, is chosen as the primary material. Although this material is usually used as a blown molding resin, it has relatively higher melt flow index and higher density than some film grade HDPE resins. Therefore, this material was expected to have better processability and lower permeability. A blown film grade LDPE, Dow 640 I, was selected as a reference material.

The choice of mica was due to its expected high aspect ratio (HAR) [31]. Three mica grades were chosen as additives to improve the barrier properties of the polyethylene films. These micas have different sizes (average diameter of Mica200HK: 45 μm, vs. that of Mica325HK: 21 μm) and different surface treatments (200HK vs. 200PE). (see Table 3.2).

4.1.2 Compounding

The twin screw extruder appeared very effective on mixing and dispersing the micas in the resin. The extrudates with 10 wt% of the various micas in either LDPE or HDPE

appear uniform with a dark brown color. All the extrudates are much stiffer than the unfilled resins at the die exit. This could be attributed to the faster rate of heat transfer through the addition of mica and the increase in the modulus of the composites. The LDPE/Mica composite was easier to extrude and pelletize than the HDPE/Mica composites.

4.2 Materials Characterization

4.2.1 Apparent Shear Viscosity

The shear viscosity was measured in the range from 100 to 1000 s^{-1} assumed to correspond to shear rates found in blown film extrusion. Figures 4.1 through 4.5 are the plots of shear viscosity as a function of shear rate for different polyethylene/Mica composites all in pellet form. All the PE/Mica composites have slightly higher viscosity than the pure resin within the measured shear rate range. The shear viscosity of the HDPE/Mica325HK composite appears to be the largest among the HDPE/Mica composites under the same conditions (Figure 4.1) perhaps due to the higher surface area of this finer mica grade resulting in enhanced interactions with the matrix. The shear viscosity of HDPE/Mica composites increases somewhat with increasing weight percentage of mica. For example, at the shear rate of 100 s^{-1}, the viscosities increased 3%, 6%, and 13% as the weight percentage of Mica325HK in HDPE are 5%, 7.5%, and 10%, respectively (see Table 4.1). This is in agreement with the general theory that the addition of inert solid particles to a polymer will increase the melt viscosity [33]. The viscosity of the HDPE/Mica200HK composite did not change significantly by increasing the mica concentration from 5 wt% to 7.5 wt% (Figure 4.4). For mica flakes of the same

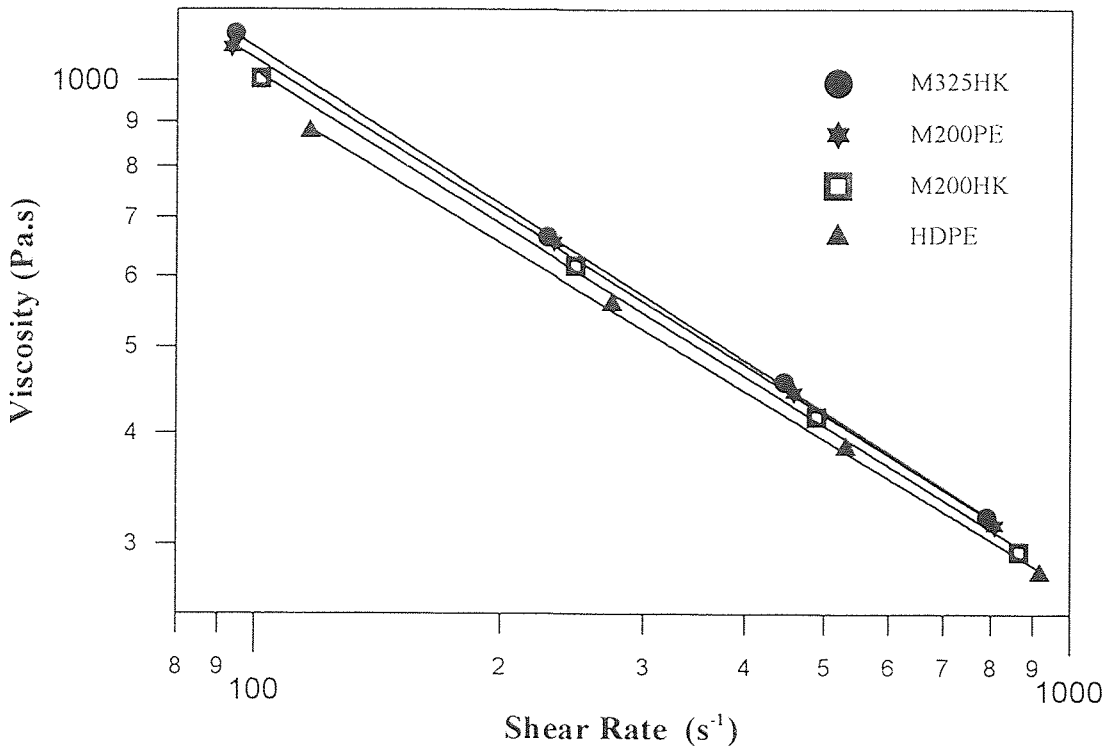

Figure 4.1 Effect of different micas (10 wt%) on the viscosity of HDPE at 230°C

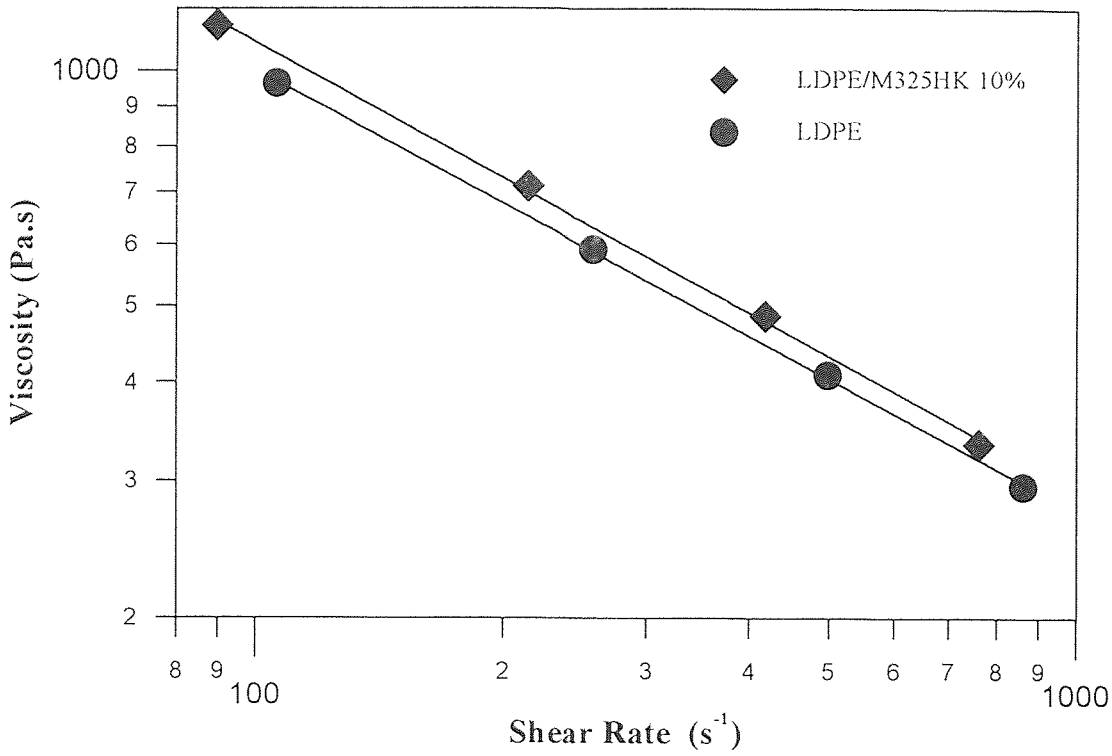

Figure 4.2 Effect of Mica325HK on the viscosity of LDPE at 190°C

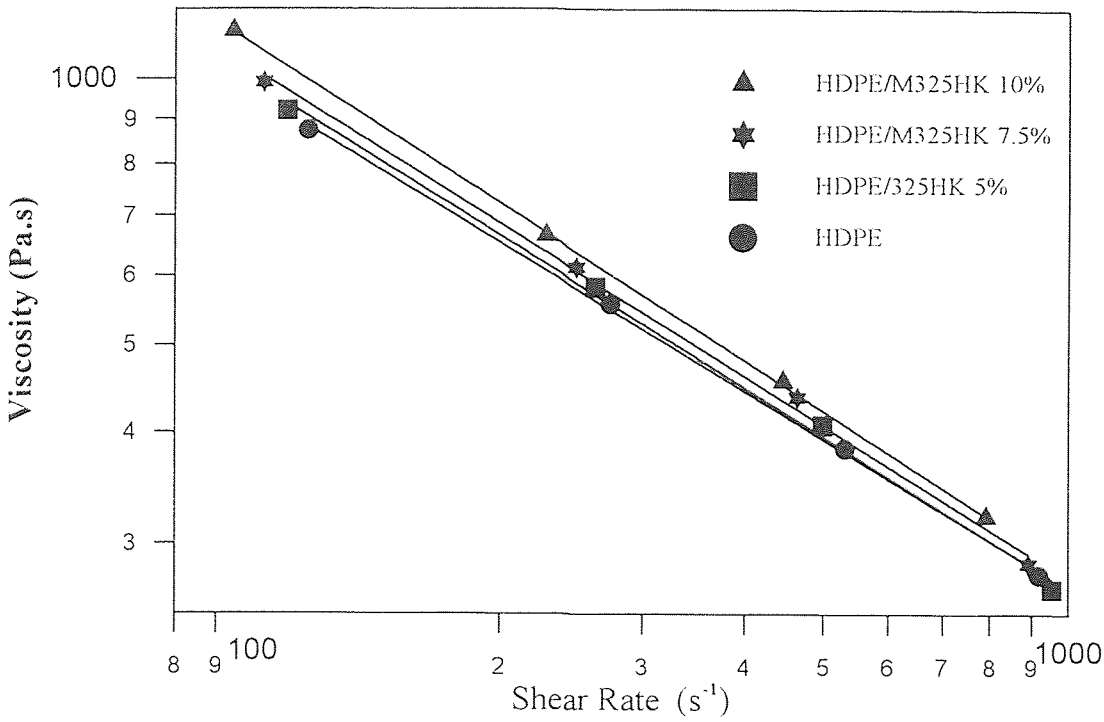

Figure 4.3 Effect of Mica325HK on the viscosity of HDPE at 230°C

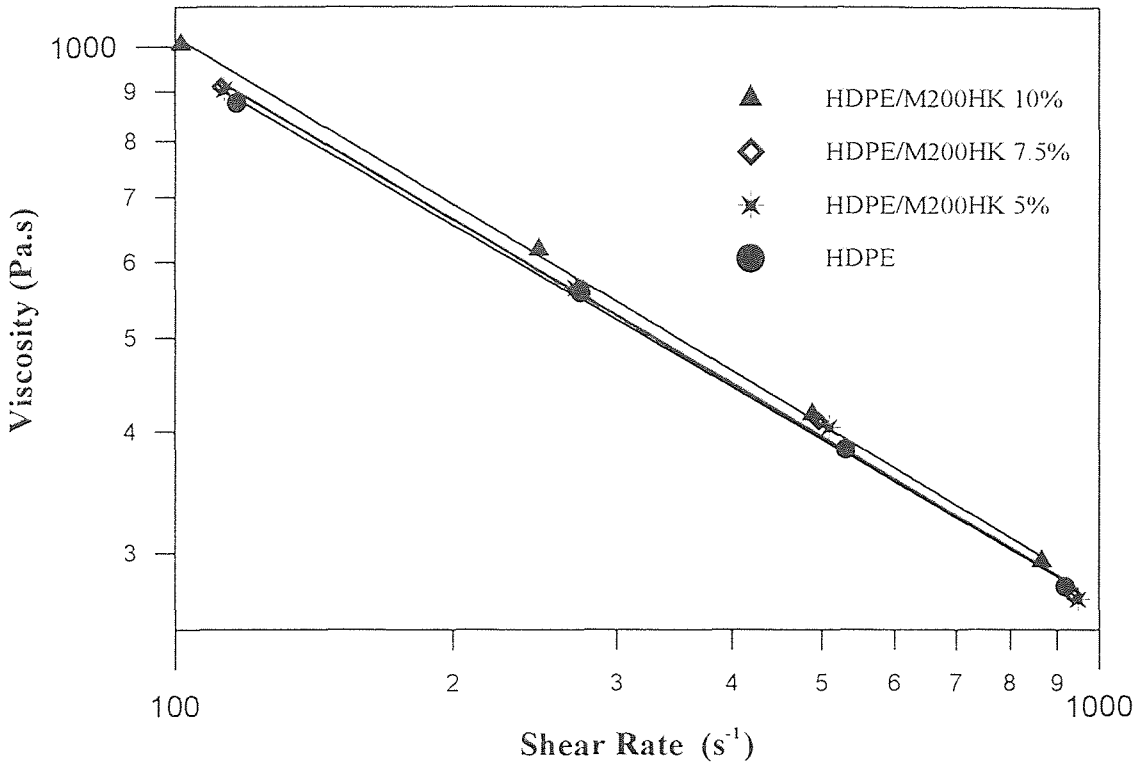

Figure 4.4 Effect of Mica200HK on the viscosity of HDPE at 230°C

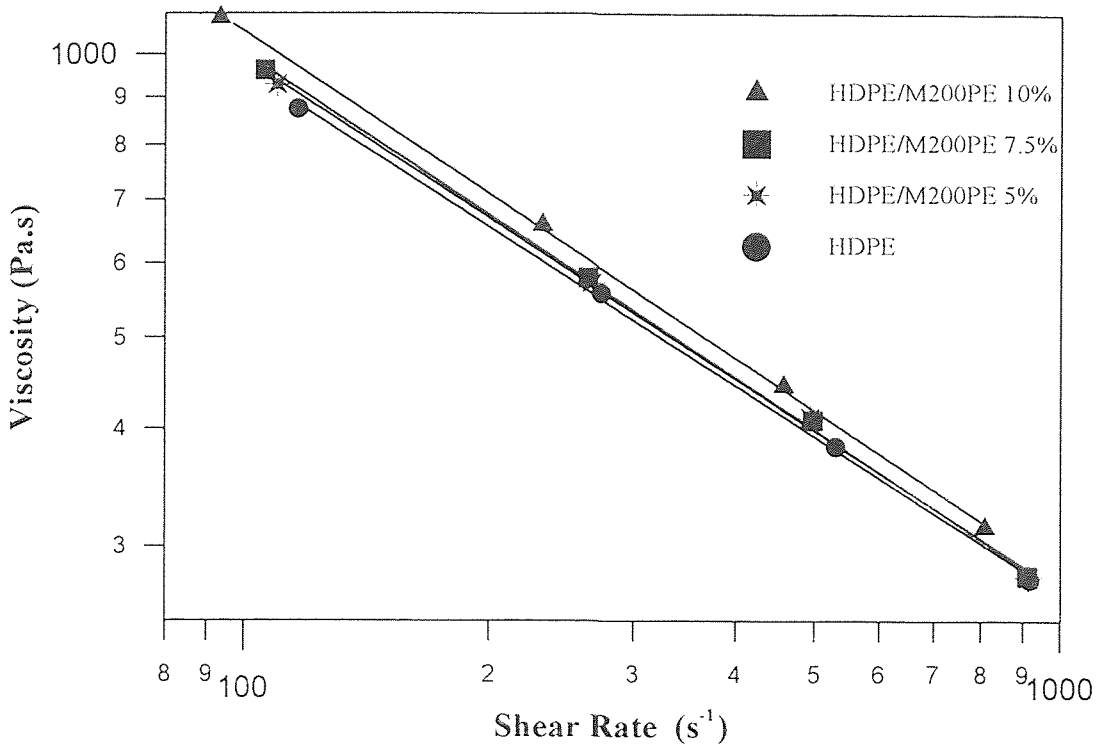

Figure 4.5 Effect of Mica200PE on the viscosity of HDPE at 230°C

Table 4.1 Shear Viscosities of PE and PE/Mica Composites (Pellets and Films)

Materials		Shear viscosity (Pa.s) at 230°C			
Compositions	Mica wt%	@100 s^{-1} shear rate		@500 s^{-1} shear rate	
		Pellet	Film	Pellet	Film
LDPE*	0	1072	1002	438	406
LDPE/Mica325HK *	10	1142	1086	465	433
HDPE	0	963	999	393	406
HDPE/Mica325HK	5	990	1142	396	448
	7.5	1020	1016	407	412
	10	1091		424	
HDPE/Mica200HK	5	986	1010	398	409
	7.5	983	1009	397	405
	10	1024		408	
HDPE/Mica200PE	5	988	1040	399	418
	7.5	1005	1006	402	404
	10	1060		420	

* The shear viscosities were measured at 190°C.

nominal size, the viscosity of HDPE/Mica200HK is slightly lower than that of HDPE/Mica200PE at all the loading levels. Further analysis of this observation is not possible in the absence of information related to the nature of the surface treatment used in the production of 200PE. Also in Table 4.1, viscosity data of the materials after being processed into blown films are included. The viscosities of the HDPE films are somewhat higher than those of the equivalent pellets. However, for LDPE and its compounds, viscosities are somewhat higher for the pellets which were exposed to fewer processing steps.

The above results confirm the complexity of the rheological properties of the polymer melts filled with nonspherical rigid particles. In addition to factors, such as the weight fraction, shape, size and size distribution of the particles, orientation at high shear rates, the state of dispersion of the particles (well-dispersed state or agglomerated state), and matrix-filler interaction, that are known to influence the rheological properties of the polymer/filler composites [33], it appears that the number of processing steps has also a measurable effect.

4.2.2 Melt Elasticity Index

Melt Elasticity Index may be defined as the amount of recovery after a specific period of time from the shear deformation imposed on the polymer melt, and could be related to important parameters during processing such as die swell and melt strength [34].

The recoverable strains at 5 seconds, 20 seconds, and equilibrium are listed in Table 4.2 as MEI_5, MEI_{20}, and MEI_∞ respectively. Only films were used for these measurements. The equilibrium times for strain recovery are also listed in Table 4.2. It

Table 4.2 Melt Elasticity Indices of PE and PE/Mica Composites Blown Films

Materials		MEI (strain unit) (190°C)		
Compositions	Mica wt%	MEI_5	MEI_{20}	MEI_∞
LDPE	0	1.10	2.04	2.17
LDPE/M325HK	10	2.04	2.43	2.72
HDPE	0	1.88	2.47	4.00
HDPE/M325HK	5	2.66	3.41	5.34
	7.5	1.91	2.49	4.03
HDPE/200HK	5	1.88	2.47	3.69
	7.5	1.96	2.54	3.94
HDPE/200PE	5	1.99	2.60	4.26
	7.5	1.90	2.45	3.88

has been suggested that MEI_{20} is considered as the standard value [35]. The MEI_{20} increases 20% by adding 10 wt% of mica in the LDPE resin. However, the results of the MEI_{20} for HDPE/Mica composites are quite different. By adding 5 wt% of Mica325HK in HDPE, the MEI_{20} increases 38%, but with a further increase in the Mica325HK concentration to 7.5 wt%, the MEI_{20} decreases down to almost the same value as for unfilled HDPE. Mica200PE appears to have the same tendency as Mica325HK although differences are only marginal. The MEI results for HDPE/Mica200HK are different. For the HDPE/5 wt% Mica200HK composite, MEI_{∞} appears to be lower than for pure HDPE while MEI_5 and MEI_{20} are the same as those of pure HDPE. For the HDPE/7.5 wt% Mica200HK composite, however, MEI_5 and MEI_{20} are not much different than unfilled HDPE.

It was expected that melt elasticity index values could be correlated with processability, the latter decreasing with increasing mica content for the HDPE compounds as shown below. However, the similarity of the measured values to those of unfilled HDPE, even at 7.5 wt% mica, suggests that MEI measurements alone could not be used as a criterion of processabilities.

4.3 Blown Film Extrusion

LDPE Dow 640 I has very good processability on the blown film extrusion line, even with 10 wt% of Mica325HK. HDPE AD60-007 is also easy to process in the blown film line. However, as the mica loadings increase, the processability of HDPE/Mica composites decreases. Because of the small amount of materials available, the objective

in processing was to obtain film products under the best possible conditions (see Table 3.4). Under such conditions processability was overall reasonably good.

The composites with 5 wt% of mica could be processed at very close the blow-up ratio of the unfilled HDPE at a lower haul-off speed. By increasing the weight fraction of mica to 7.5%, both blow-up ratio and haul-off speed had to be reduced to produce satisfactory films. The composites with 10 wt% mica could not be used to make films. The lower the blow-up ratio and the haul-off speed, the thicker the film. This is one of the reasons for the difference in thickness of the films besides the mica loading. The processability of blown film can be roughly explained by a synthesized parameter, draw ratio as defined in Chapter 3. The draw ratio is reduced with increasing difficulty of processing. For the HDPE/Mica composites, the change of processability of blown film with increasing mica loadings can also be related to changes in shear viscosity under those conditions. The higher the mica fraction, the higher the shear viscosity (as well the elongational viscosity), and the poorer the processability.

Another reason for the reduction in processability could be related to the thermal conductivity of the composites. The increase in the weight fraction of mica increases the thermal conductivity of the composite [36], therefore, the frost line is lowered. Decreasing the distance between the die lips and the frost line, makes the stress profile steep. The composite melt bears large stresses between the die lips and the frost line. In order to avoid blowing out, the stress applied on the composite melt has to be lowered. This was done by reducing the blow-up ratio and the haul-off speed. The thickness of the film was increased accordingly, and the uniformity of the thickness is therefore, limited at these processing conditions.

An additional reason for reduction of processability may be related to an essential rheological parameter which is the elongational viscosity. Non-Newtonian behavior occurs when the tensile stress imposed on the melts is above 10^3 Pa for polyethylenes: branched PE tension-stiffens and therefore is easier to process; linear PE tension-thins [23]. When there are sites which can cause stress concentration to the melt, tension-stiffening eliminates these spots and tension-thinning results in melt necking in the regions where stress concentration exists. The presence of micas in extrudates below the frost line may act as sites of stress concentration. For the HDPE/mica composites, the increasing difficulty in processing is obvious as the weight percentage of mica increases.

As expected, the blend of HDPE/LDPE (1:1) is easier to process than HDPE alone. However, the addition of 10 wt% Mica325HK into the compound, produces innumerable fish eyes along the machine direction during blowing and made the film unacceptable.

4.4 Morphology of Blown Films

4.4.1 Transmission Optical Microscope Study

The morphology of the top surfaces and a few underneath layers of the blown films can be observed under transmission optical microscope. Micrograghs in Figure 4.6 and Figure 4.7 show three kinds of mica in HDPE films under the magnification of 400X. In these pictures the broad faces of micas are aligned parallel to the film surface, which could be contributed to the high shear stress applied on the film surfaces during processing; the dispersed phase (mica) is well distributed in the polyethylene matrix. There are some differences in these pictures: the particle size and its distribution. The average particle sizes estimated from 50 - 60 particles are listed in Table 4.3. The observed mica size

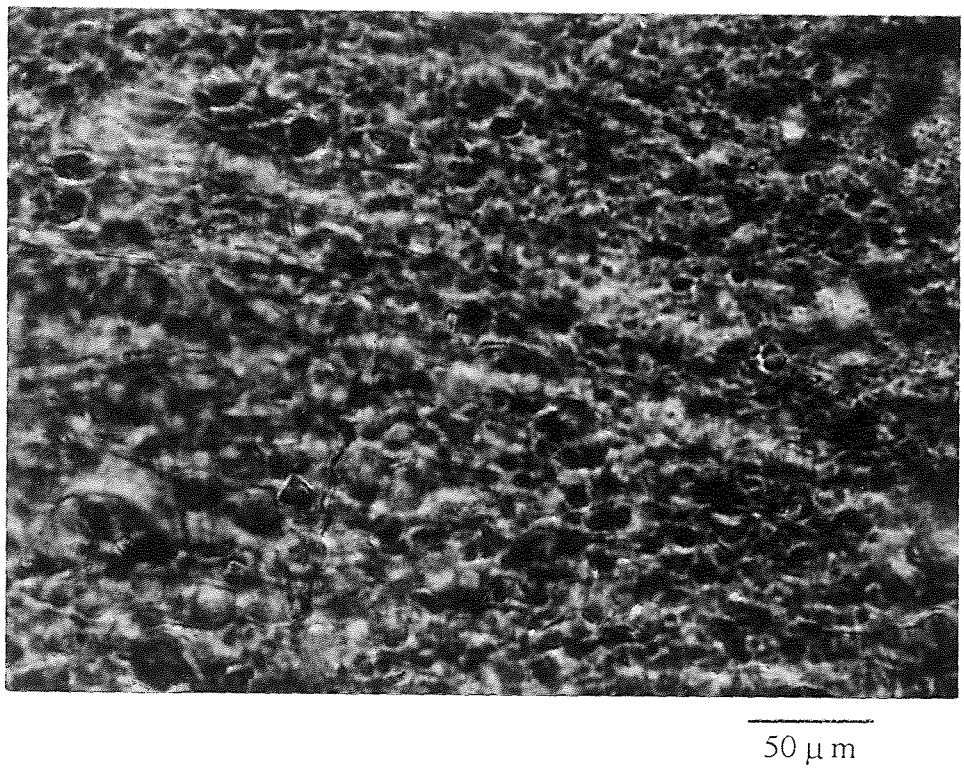

Figure 4.6 TOM micrograph showing morphology of the surface of HDPE/5 wt% Mica325HK composite blown film (400 X)

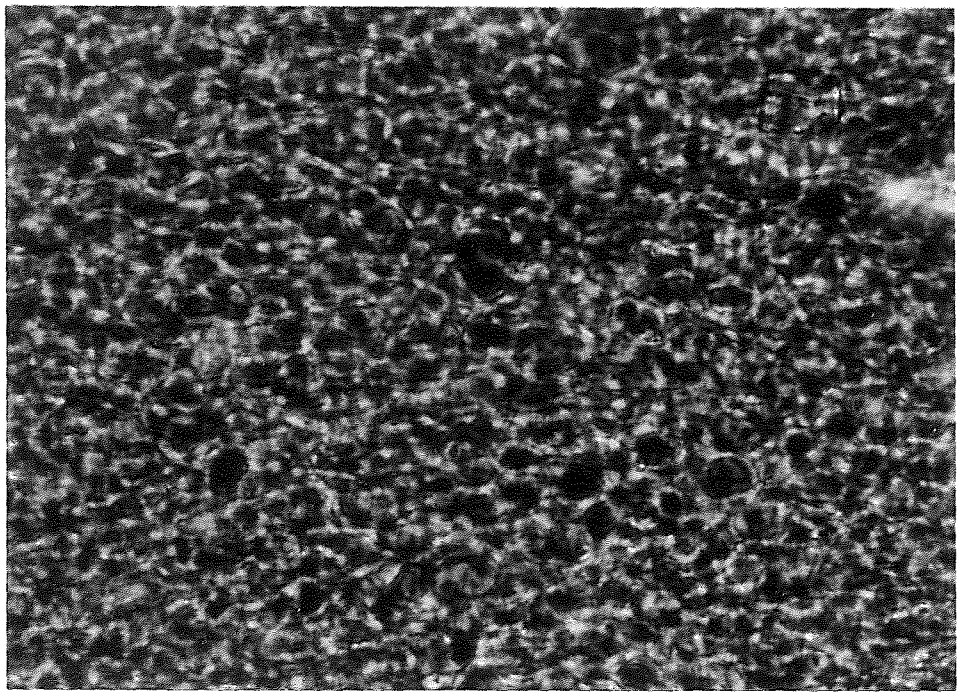

(a) HDPE/5 wt% Mica200HK (400 X) 50 μm

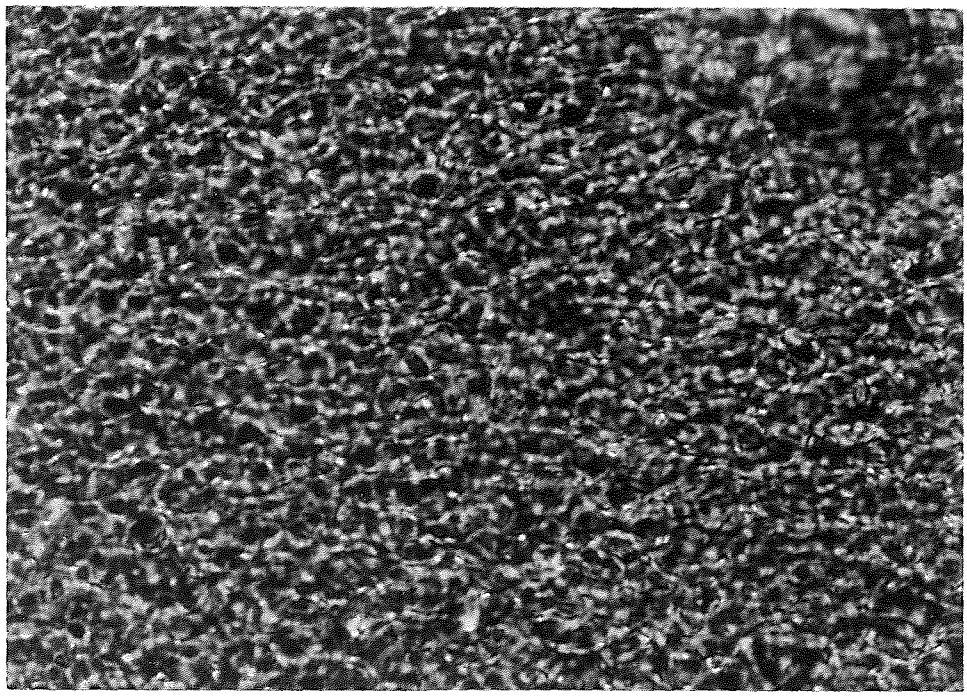

(b) HDPE/5 wt% Mica200PE (400 X) 50 μm

Figure 4.7 TOM micrographs showing morphology of the surfaces of HDPE/mica composites blown films

Table 4.3 Dimensions and Distribution of Mica Flakes in Blown Films

Mica	Wt. (%)	Matrix	Average diameter (μm)	Average thickness (μm)	Average aspect ratio	Average distance between layers (μm)	
						Measured	Calculated
325HK	5	HDPE	12	0.5	24	11.5	6.7
200HK	7.5	HDPE	15	1	15	10.6	7.9
200PE	7.5	HDPE	12	1	12	9.3	6.6

from the blown films indicates that Mica325HK has about the same average particle size as that of Mica200PE and appears smaller than that of Mica200HK. The particle size distribution of Mica200PE is rather uniform, while a much broader particle size distribution is observed in PE/Mica325HK films.

Changes in particle size and its distribution could be attributed to the processes of compounding and extrusion. It is easier to break a larger rigid particle (e.g. 200HK or 200PE) in the elliptical shape. For Mica200PE, better adhesion between the polyethylene matrix and mica could be expected, therefore, the stress transferred to mica is more effective and uniform. In estimating flake diameter, it is also possible that the broad faces of micas may not be aligned parallel to the film surfaces, so that the size of mica shown in the micrographs can be misleading. The other sides which are vertical to the surfaces, i.e., the cross-section of the film, were observed by SEM as shown below.

4.4.2 Scanning Electron Microscope Analysis

The microstructures of the cross-section of the polyethylene/mica blown films were studied under Scanning Electron Microscope (SEM). Figure 4.8 and Figure 4.9 show three kinds of mica in HDPE films. Mica flakes are well oriented with the broad faces parallel to the film surfaces, and overlapping discontinuous mica layers are formed. However, some Mica200HK flakes appear less oriented. The fracture surfaces of HDPE/Mica200HK and HDPE/Mica200PE are different from those of HDPE/ Mica325HK. The thickness of Mica325HK is smaller than that of either Mica200HK or Mica200PE. The average thickness of these three types of mica estimated from about 15 particles are listed in Table 4.3.

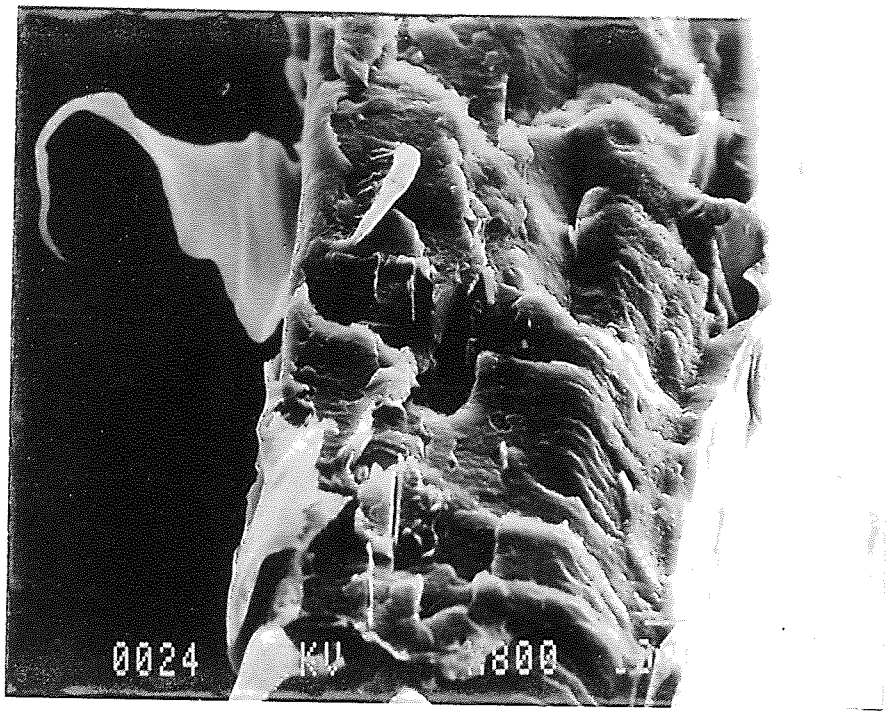

Figure 4.8 SEM micrograph showing morphology of the cross-section of HDPE/5 wt% Mica325HK composite blown film

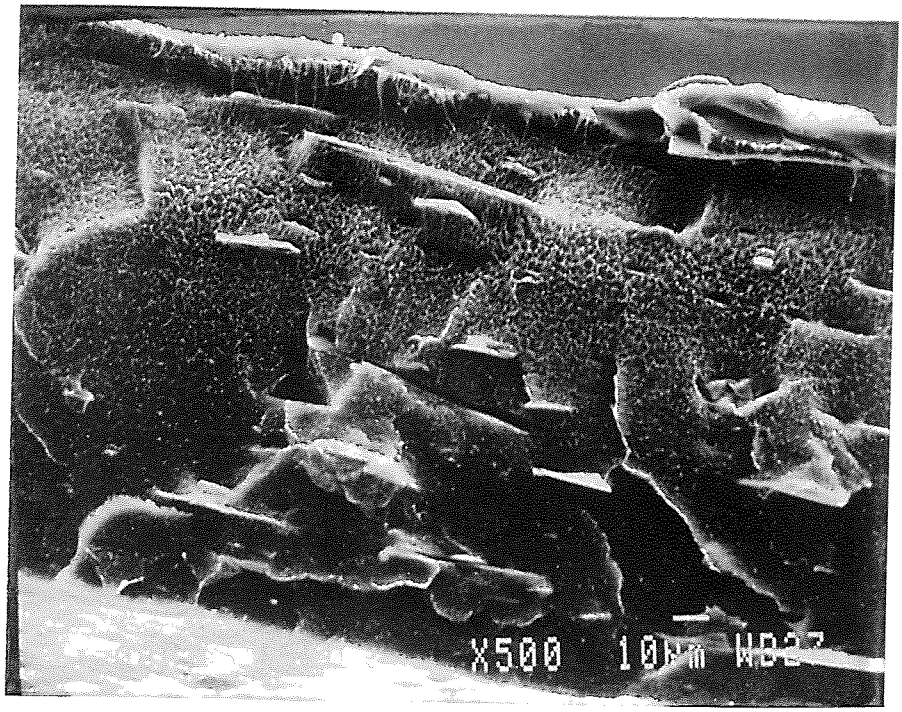

(a) HDPE/5 wt% Mica200HK

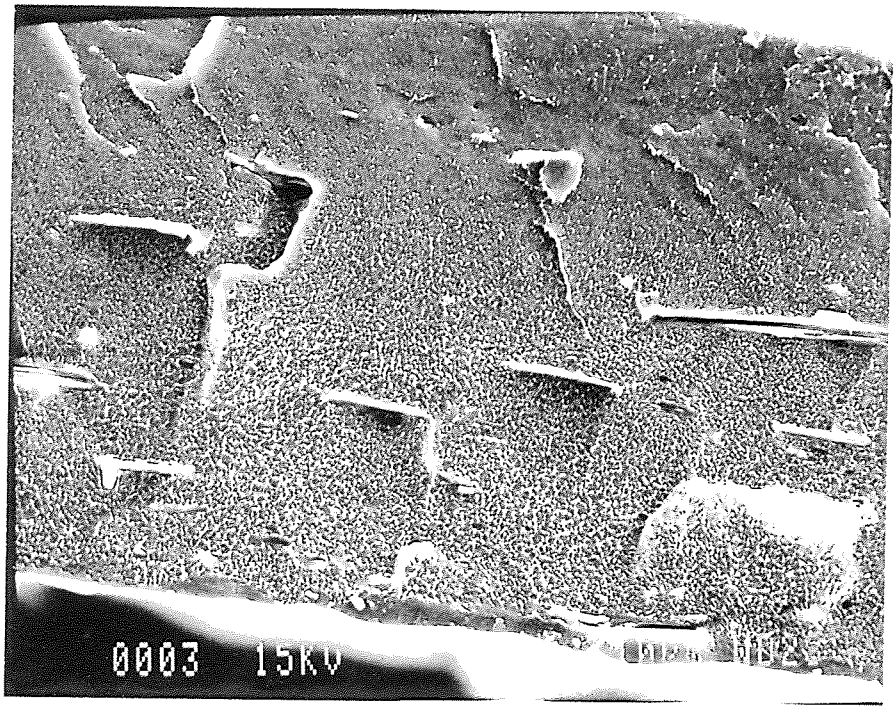

(b) HDPE/5 wt% Mica200PE

Figure 4.9 SEM micrographs showing morphology of the cross-section of HDPE/mica composites blown films

From the average thickness (l) and average diameter (d) estimated above, the aspect ratio of micas, a, is defined as [33]:

$$a = \frac{d}{l} \qquad (4.1)$$

The aspect ratio of three types of mica are also listed in Table 4.3. For example, Mica325HK has an average diameter of 12 μm and an average thickness of 0.5 μm, its aspect ratio is 24.

The distance between the nearest mica layers can be obtained by calculating the thickness of the film divided by the number of mica layers observed from the micrographs. This distance can also be estimated through the physical properties of both mica and the matrix using the following procedures (see Figure 4.10):

First, the weight fraction of mica, w_f, can be converted to a volume fraction, ϕ_f, using the following equation:

$$\phi_f = \frac{w_f \rho_m}{w_f \rho_m + (1 - w_f)\rho_f} \qquad (4.2)$$

where ρ_m and ρ_f are the densities of the matrix and the fillers respectively.

Second, assuming the size of mica flakes is the same, the total number of mica flakes, m, in a unit volume of PE/mica composite can be calculated as:

$$m = \frac{\phi_f}{V} \qquad (4.3)$$

where V is the volume of one mica flake, which can be simplified as in a circular shape, therefore

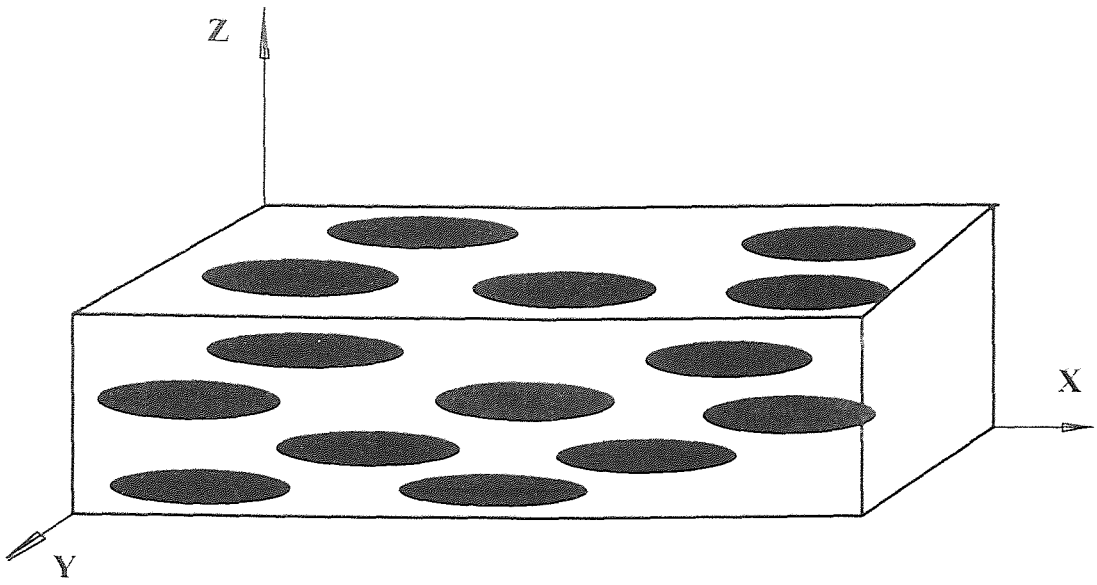

X: Machine direction (MD)
Y: Transverse direction (TD)
Z: Film thickness direction

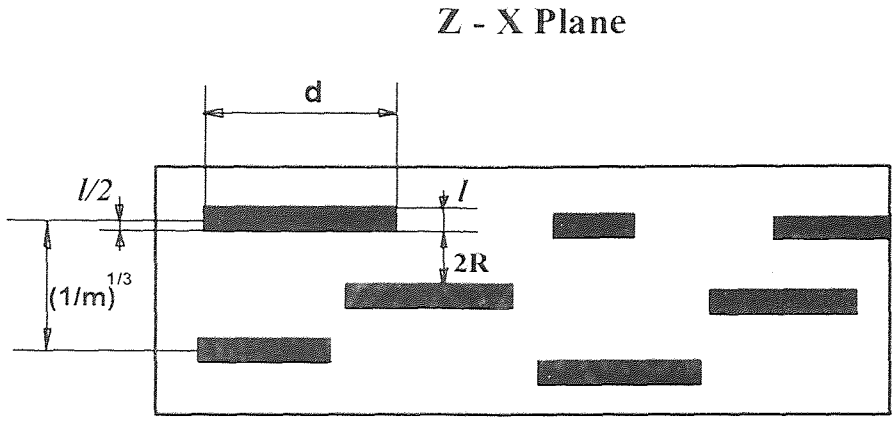

Figure 4.10 Schematic sketch of mica dimensions and distribution in blown film

$$V=\frac{\pi}{4}ld^2 \qquad (4.4)$$

The volume occupied by one mica flake is 1/m, and the length of each side of the cubic volume is $(1/m)^{1/3}$. The value $(1/m)^{1/3}$ should be the distance between the neighboring mica layers. However, this value is smaller than the diameter of mica due to the high aspect ratio of mica flakes. This means that the mica flakes with the broad face in the same direction cannot be assigned to every assumed unit in the same plane. It is reasonable to assume that they are split into two layers overlapped at the thickness direction. The average distance (2R) to the nearest neighbor layer can be calculated as:

$$2R=\frac{(1/m)^{\frac{1}{3}}-2l}{2} \qquad (4.5)$$

For instance, for the HDPE/5 wt% Mica325HK film, the volume fraction of Mica325HK is 0.017, the volume of one Mica325HK flake is approximately 56.5 μm^3 (l=0.5 μm, d=12 μm), so that the number of mica flakes in 1 mm^3 is about 300,000. The calculated average distance between the nearest mica layers is about 6.7 μm.

The estimated values of average distance to the nearest neighbor are smaller than those measured from the SEM micrographs. This may be attributed to the simplifications such as the shape of mica and the assumed packing of the mica flakes in the film.

4.5 Mechanical Properties of Blown Films

All tensile properties of blown films are measured and calculated according to the ASTM D882-91 standard. The yielding stress (σ_y), the stress at break (σ_b) and elongation (ε_b) at break, the elastic modulus (E), as well as the standard deviation (estimated) for all

these measurements are listed in Tables 4.4 and 4.5 for the machine and transverse directions. Films of LDPE and its composite are tested at a higher strain rate than HDPE and its composites. Therefore, these properties can not be directly compared.

4.5.1 Tensile Stress

The tensile stress at break for blown films made of various compositions are shown in Figure 4.11. The ultimate tensile stress values of unfilled polyethylenes are higher than those of their composites. For blown films with all three types of mica, it seems that the stress values go through a valley, then tend to rise at both machine direction (MD) and transerse direction (TD) as the weight percentage of mica increases. This phenomenon could be caused by the effect of the mica presence on the orientation of the polyethylene molecules and the assumed increasing orientation of mica with increasing its weight fraction in the composites.

For the films of LDPE and its mica composite, the tensile stress at break in the machine direction is higher than that in the transverse direction. On the contrary, almost all the values of tensile stress at break for the films of HDPE and its mica composites in the machine direction are lower than those in the transverse direction. The tensile stress at yield has a similar trend to that of the stress at break. The yield stress of HDPE/5 wt% Mica composites, however, has a different tendency when compared to the tensile stress at break. The yield stress for these composites in the machine direction is higher than that in the transverse direction (see Figure 4.12).

Almost all films have higher yield stress than tensile stress at break in both machine and transverse directions except for the LDPE samples, but the differences are less signi-

Table 4.4 Mechanical Properties of Blown Films in the Machine Direction

Material	Mica wt%	σ_y(MPa) average	dev.	σ_b(MPa) average	dev.	ε_b(%) average	dev.	E (MPa) average	dev.
LDPE	0	9.6	0.05	14.4	0.43	230	2.1	212	13.1
LDPE/ M325HK	10	10.1	0.05	14.3	0.27	155	4.6	277	16.5
HDPE	0	26.3	0.34	20.0	1.56	800	28.3	628	51.2
HDPE/ M325HK	5	18.8	0.03	14.7	0.16	67.0	0.7	984	26.9
	7.5	23.7	0.16	19.9	0.79	20.5	0.6	1510	55.9
HDPE/ M200HK	5	20.0	0.20	17.1	0.08	21.0	4.2	1057	29.0
	7.5	21.6	0.03	17.3	0.27	17.2	0.1	1241	47.6
HDPE/ M200PE	5	14.6	0.09	13.0	0.48	39.6	1.7	934	49.0
	7.5	24.6	0.15	19.0	0.69	17.2	0.2	1346	69.0
HDPE/ LDPE	0	16.1	0.13	16.2	0.37	402	25.0		
HD/LD M325HK	10	13.4	0.23	12.8	0.29	16.5	0.4		

Table 4.5 Mechanical Properties of Blown Films in the Transverse Direction

Material	Mica wt%	σ_y(MPa) average	dev.	σ_b(MPa) average	dev.	ε_b(%) average	dev.	E (MPa) average	dev.
LDPE	0	11.7	0.27	12.9	0.34	569	17.0	329	15.1
LDPE/ M325HK	10	9.4	0.54	7.9	0.17	65	0.4	347	8.2
HDPE	0	31.3	1.18	28.7	0.49	6.0	0.7	921	91.5
HDPE/ M325HK	5	14.2	0.38	13.0	0.45	3.9	0.0	1105	15.9
	7.5	25.1	1.02	24.5	1.01	3.1	0.1	1901	29.7
HDPE/ M200HK	5	19.6	0.57	18.9	0.30	2.2	0.0	1293	44.8
	7.5	25.8	0.15	25.8	0.15	3.6	0.1	1832	105.5
HDPE/ M200PE	5	14.5	0.61	14.5	0.61	1.5	0.1	1069	78.6
	7.5	23.6	0.73	23.0	0.53	2.5	0.0	1625	65.5
HDPE/ LDPE	0	17.1	0.43	12.7	0.42	60.0	2.5		
HD/LD M325HK	10	12.2	0.16	10.9	0.09	2.5	0.0		

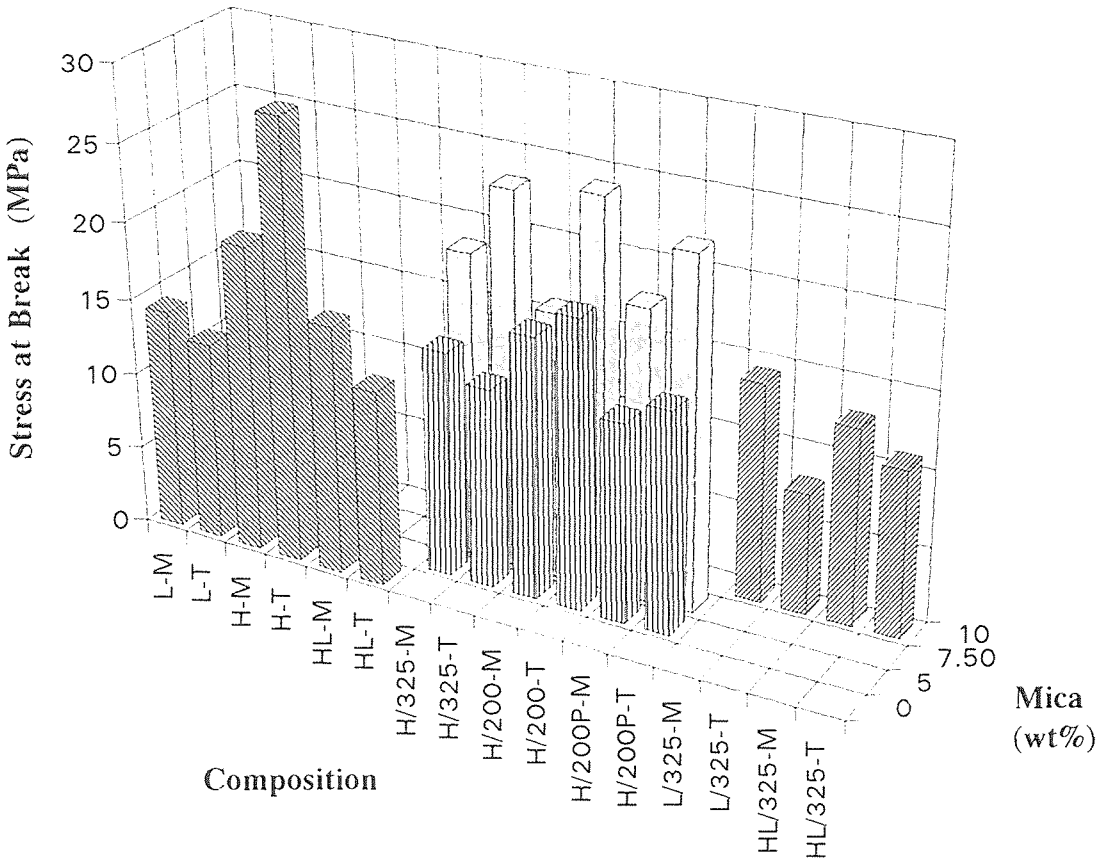

Figure 4.11 Stress at break as a function of polyethylene/mica composition and mica weight percentage. (L=LDPE, H=HDPE, M=machine direction, T=transverse direction)

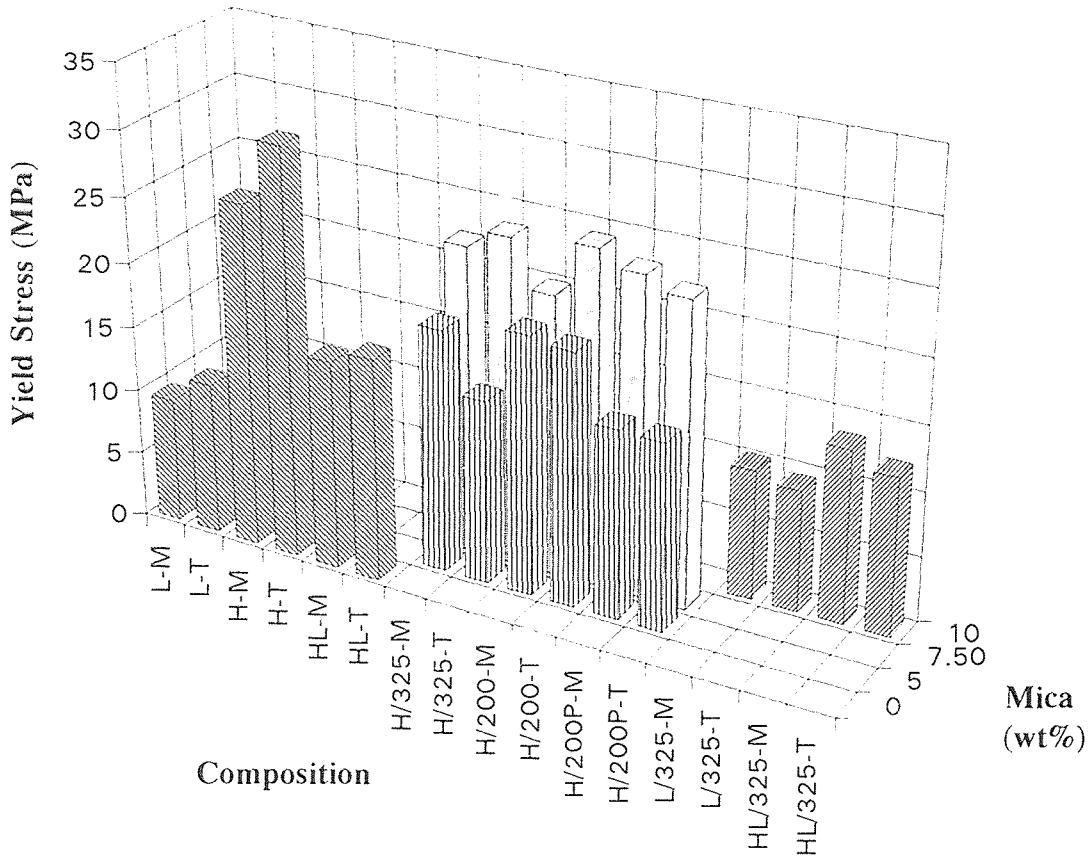

Figure 4.12 Yield stress as a function of polyethylene/mica composition and mica weight percentage. (L=LDPE, H=HDPE, M=machine direction, T=transverse direction)

ficant in the transverse direction. Depending on the particular film and the process conditions used in blowing (haul-off speed and blow-up ratio), different degrees of biaxial stretching were obtained; these are manifested in the different ratios of stress values in the machine vs. transverse direction. Differences then, are due to both molecular and filler orientation. With respect to the anticipated enhanced properties for the 200PE films as a result of increased adhesion, such effects are not evident from the values of Tables 4.4 and 4.5.

4.5.2 Elastic Modulus

The elastic modulus in both machine and transverse directions are increasing with increasing mica concentration as shown in Figure 4.13. The increase is the fastest for HDPE/Mica325HK composites in the machine direction; for example, the modulus of HDPE/7.5 wt% Mica325HK is 2.4 times that of the unfilled HDPE. On the other hand, the modulus of LDPE/10 wt% Mica325HK increases only 31% in the machine direction and 5% in the transverse direction as compared with the modulus of the unfilled LDPE.

The elastic modulus of all films in the transverse direction is higher than that in the machine direction. This difference could be caused by the amorphous phase in which the orientation is distributed more uniformly in the transverse direction [37]. The increase in modulus involving high aspect ratio fillers which are assumed to be perfectly aligned to the direction of stress applied can be explained successfully using a simple shear lag theory [23] which is generally applied to discontinuous fibers:

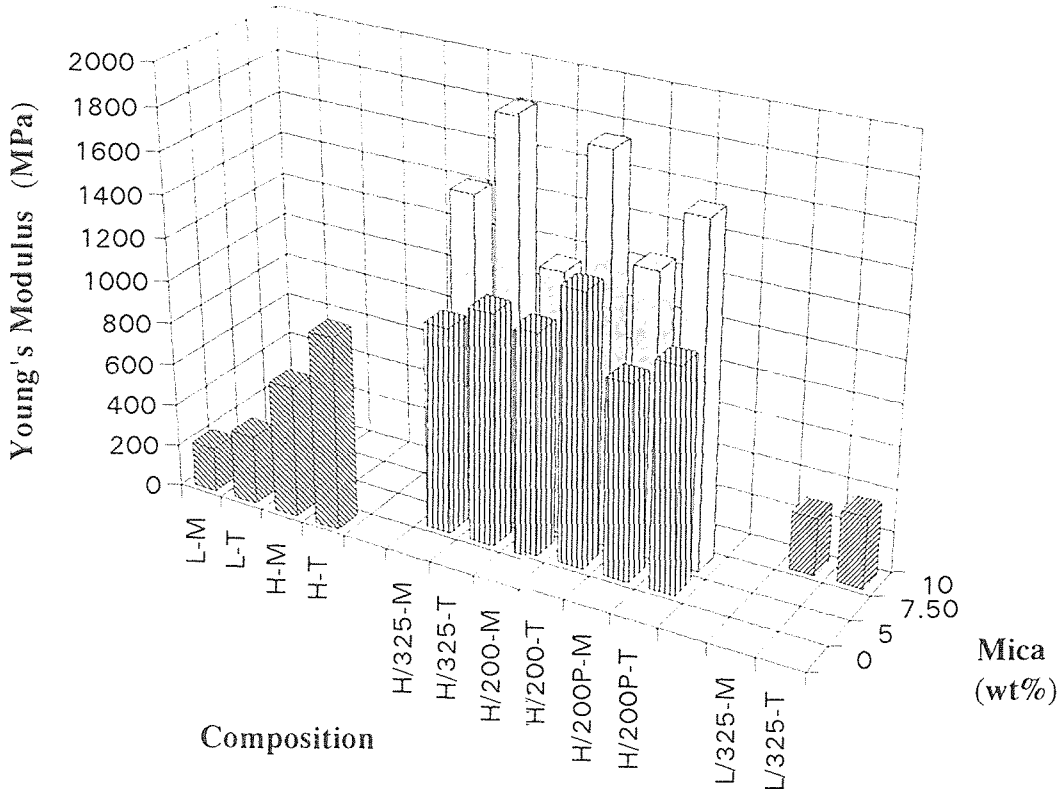

Figure 4.13 Young's Modulus as a function of polyethylene/mica composition and mica weight percentage. (L=LDPE, H=HDPE, M=machine direction, T=transverse direction)

$$E_c = \eta_1 \phi_f E_f + (1 - \phi_f) E_m \qquad (4.6)$$

where E_c, E_f, and E_m are the moduli of composite, fillers, and matrix respectively. ϕ_f is the volume fraction of the filler, and η_1 is a factor which corrects the modulus of filler considering the length of the filler and is given by:

$$\eta_1 = 1 - \left[\frac{\tanh(na)}{na}\right] \qquad (4.7)$$

where a is the aspect ratio of the filler, and n is a dimensionless constant:

$$n = \sqrt{\frac{2G_m}{E_f \ln(2R/l)}} \qquad (4.8)$$

where G_m is the shear modulus of the matrix, 2R is the distance from the filler to its nearest neighbor, and l is the filler dimension in the direction of 2R. For a given composite, n decreases with increasing 2R, while 2R decreasing with increasing filler volume fraction. Therefore, n increases with increasing filler volume fraction. From the above equations, we can see that the elastic modulus of the composite depends on both the aspect ratio (a) and the volume fraction (ϕ_f) of the filler.

For example, Mica325HK has an elastic modulus of 172 GPa, is well distributed in HDPE (its elastic modulus is 628 MPa in the machine direction) and the mica volume fraction of 0.017 (5 wt%). The estimated value of 2R is 6.7 μm from Equation 4.5, and l is 0.5 μm from Table 4.3. We can also assume that the shear modulus of the matrix is one third of its elastic modulus. Substituting all the parameters into Equations 4.6 through 4.8, we get an estimated elastic modulus of 1050 MPa for the film of HDPE/5 wt% Mica325HK composite in the machine direction. The measured value of 2R is 11.5 μm

(Table 4.3), so the elastic modulus in the MD is estimated to be 987 MPa. These estimated moduli are close to the measured value which is 984 MPa in machine direction.

4.5.3 Elongation at Break

As shown in Figure 4.14, the elongation at break decreases dramatically by increasing the mica loading in HDPE. The elongation at break for unfilled HDPE is 800%, while it drops to double digits in percentage in the machine direction and single digits in the transverse direction for its composites. The addition of the rigid filler, increases the stiffness and brittleness of the polyethylene films [38]. This loss in ductility should be affected not only by the filler concentration, but also by the particle size and particle size distribution.

4.6 Permeability to Oxygen

4.6.1 Considerations for the Experiment

The experiment of measuring the permeability of the plastic films is rather difficult in practice due to the small thickness of the film. When the pressure difference reaches a certain value, the specimen is deformed to a hemispherical shape instead of the originally flat form. This increases the test area and reduces the thickness of specimen to various degrees for different materials. The test results were often not accurate and difficult to compare to each other. Furthermore, increasing the pressure difference, the film will creep after certain time and cause an increase in the permeability value. On the other hand, by applying a very small pressure gradient between the two sides of film, it will take a long time to establish steady-state and to collect the barely distinct data. The sudden

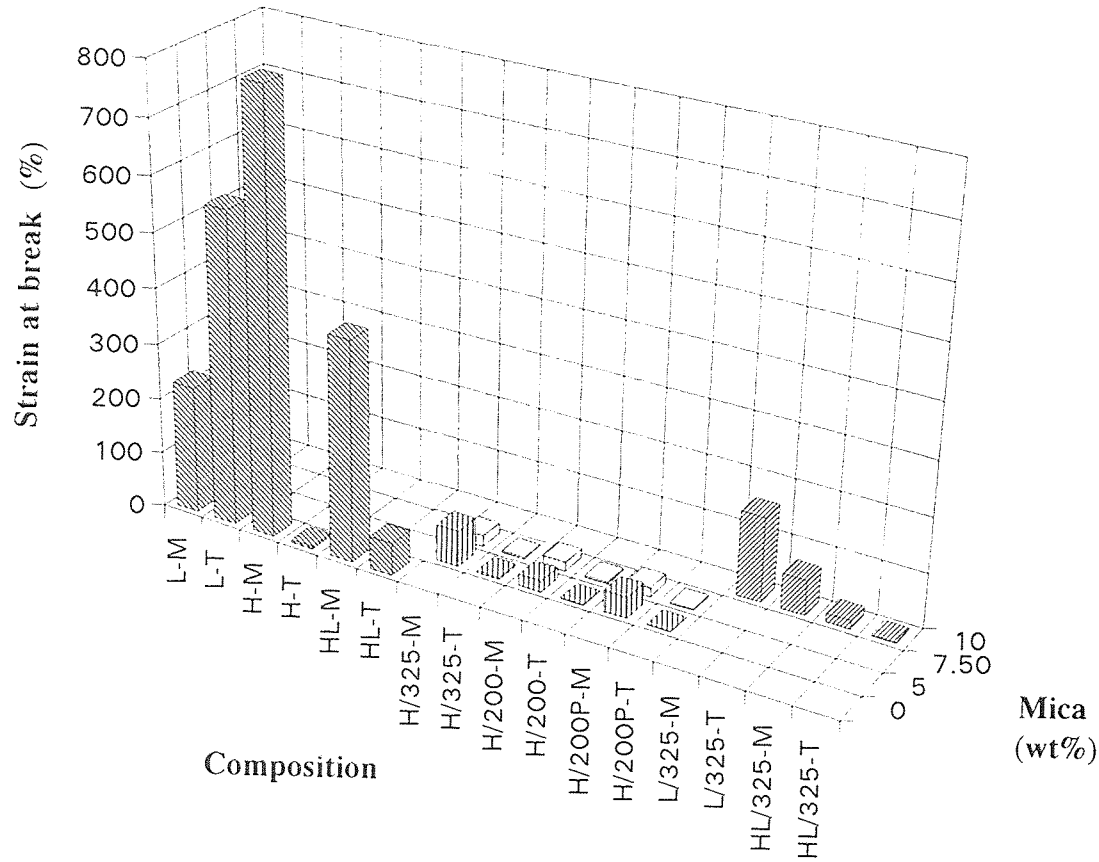

Figure 4.14 Strain at break as a function of polyethylene/mica composition and mica weight percentage. (L=LDPE, H=HDPE, M=machine direction, T=transverse direction)

breakdown of some rigid films during the test could be caused by fatigue fracture, due to the fluctuation of pressure difference resulting from temperature variations..

We needed to find the optimum pressure gradient for all films made of different materials, and to prevent the deformation of the specimens as much as possible. The latter could be done by applying several layers of filter paper to clamp the thin film in position. The non-ashing filter paper had a negligible effect on the permeability value. A range of pressure gradients, from 52 to 103 cmHg, was used in the tests.

4.6.2 The Effects of Materials Structure

All the measured values and standard deviations of permeability for polyethylene and its composites are listed in Table 4.6. Polyethylenes per se have different permeability to oxygen because of the differences in their densities. In this research, the permeability of three PE films with different densities are examined (see Figure 4.15). The permeability of PE to oxygen is reduced by increasing its density. The reason for the increase in density of PE is the increase of the crystalline regions, which is the impermeable section to oxygen [7]. For LDPE, the crystallinity is lower, so that the density is lower and the permeability is higher. For HDPE, the crystallinity is approximately 60%, the density is higher and the permeability is lower. The permeability of a film made of LDPE/HDPE (1:1) is in between the two as expected.

The addition of inorganic platelet shaped fillers into polymers can reduce the permeability of the polymer due to an increase in the migration path of the permeant. It is called "tortuosity effect", τ, as explained in Chapter 2. That is

Table 4.6 Permeability of Blown Films to Oxygen

Material	Mica wt%	Permeability (barrer) Average	Sample 1	Sample 2
LDPE	0	4.16	4.06	4.25
LDPE/M325HK	10	3.03	2.90	3.16
HDPE/LDPE	0	2.43	2.37	2.50
HDPE	0	1.98	2.03	1.92
HDPE/M325HK	5	1.71	1.67	1.75
	7.5	1.43	1.37	1.48
HDPE/M200HK	5	2.27	2.19	2.35
	7.5	2.27	2.26	2.28
HDPE/M200PE	5	3.03	2.97	3.09
	7.5	3.58	3.58	3.58

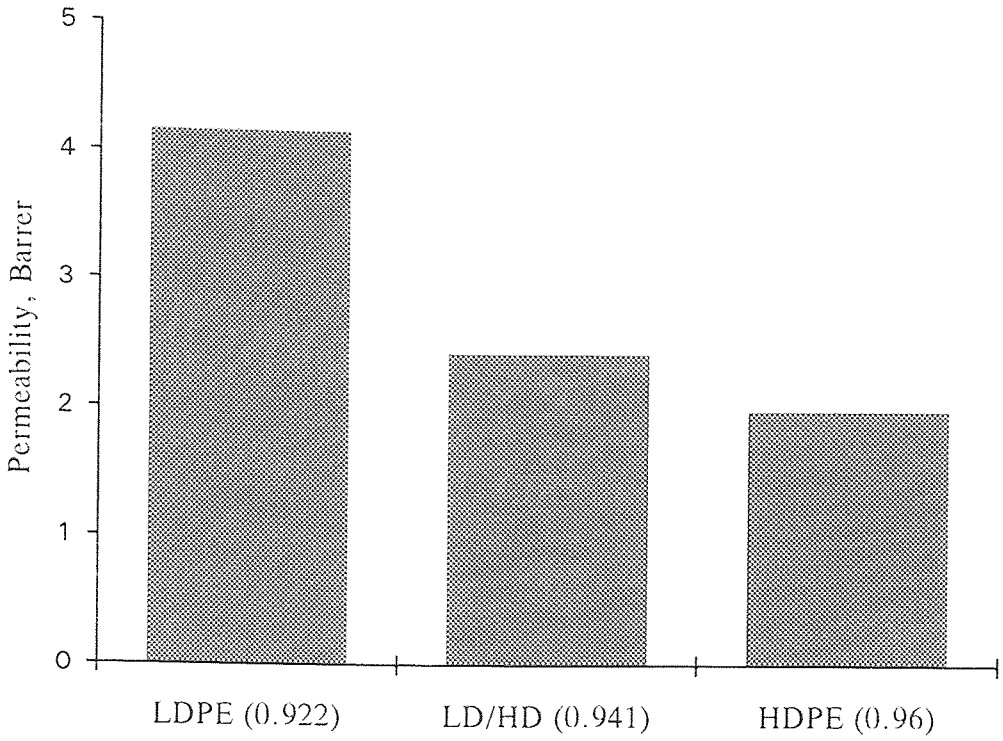

Figure 4.15 Oxygen permeability of three polyethylene films with different densities as indicated in the brackets

$$P_c = P_m \phi_m / \tau \qquad (4.9)$$

For the dispersed phase with dimensions of length d and thickness *l*, Nielsen's treatment [17] gives:

$$\tau = 1 + (d/2l)\,\phi_f \qquad (4.10)$$

where ϕ_f is volume fraction, and d/*l* is the aspect ratio of the dispersed phase. This leads to:

$$P_c = P_m \cdot \phi_m / [1 + (d/2l)\,\phi_f] \qquad (4.11)$$

where P_c and P_m are the permeability constants for the composite and polymer matrix respectively, and ϕ_m is the volume fraction of matrix phase.

The tortuosity coefficient is proportional to both the aspect ratio and the volume fraction of fillers. Mica has a relatively high aspect ratio. When the broad face of a mica flake is aligned parallel to the surfaces of the film, it can be considered that the mica flake has a higher effective aspect ratio; it is also easier to form overlapping, discontinuous layers in the polyethylene matrix when mica reaches a certain volume fraction and under proper processing conditions. In order to reduce permeability, the percentage of mica in the PE/Mica composites should be as high as possible. However, as discussed earlier, there are processability limitations due to filler concentration in the blown film process.

Mica325HK is a good example showing the effect of tortuosity on the permeability of polyethylene films. For LDPE, the addition of 3.5 volume% (10 wt%) of Mica325HK, reduces the permeability from 4.16 to 3.03 barrer (see Figure 4.16), a 27% reduction.

For HDPE, the addition of 1.7 (5 wt%) and 2.7 volume% (7.5 wt%) of Mica325HK, reduces the permeability from 1.98 barrer (pure HDPE) to 1.71 barrer and 1.43 barrer respectively (see Figure 4.17).

We can also estimate the permeability of the composites considering the tortuosity effect using Equation 4.11. The average aspect ratio for Mica325HK is 24 (Table 4.3), The estimated value of permeability for LDPE/10 wt% Mica325HK composite is 2.83 barrer, which is close to the measured value (3.03). Similarly, the estimated values of permeability for HDPE/5 wt% Mica325HK and HDPE/7.5 wt% mica325HK composites are 1.62 barrer and 1.46 barrer respectively (see Figure 4.18) vs. the measured 1.71 and 1.43 barrer.

The addition of the other two types of mica, Mica200PE and Mica200HK, however, increases the permeability of HDPE unexpectedly as shown in Figure 4.19. This could be caused by differences in their microstructures as compared to the HDPE/Mica325HK films, such as more random orientation of flakes, coarser particles [29], and possible effects on crystallinity. In general, it was observed that Mica325HK gave a smoother surface where the coarser 200 grades resulted in rougher surfaces which could result in pinholes affecting permeability.

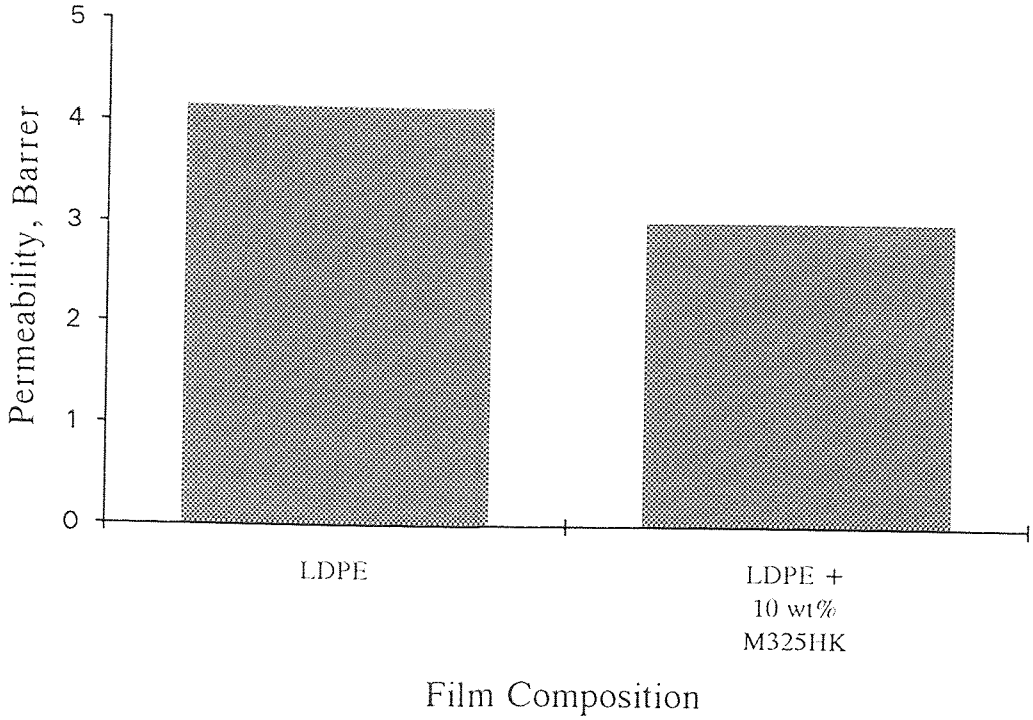

Figure 4.16 Effect of mica on the oxygen permeability of LDPE films

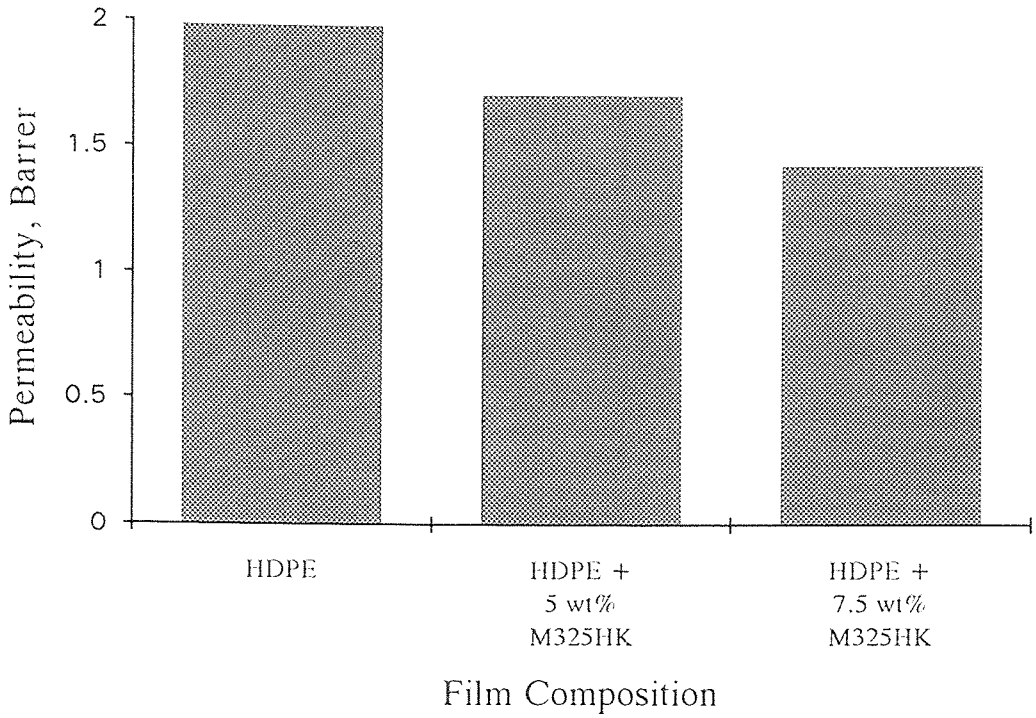

Figure 4.17 Effect of Mica325HK on the oxygen permeability of HDPE films

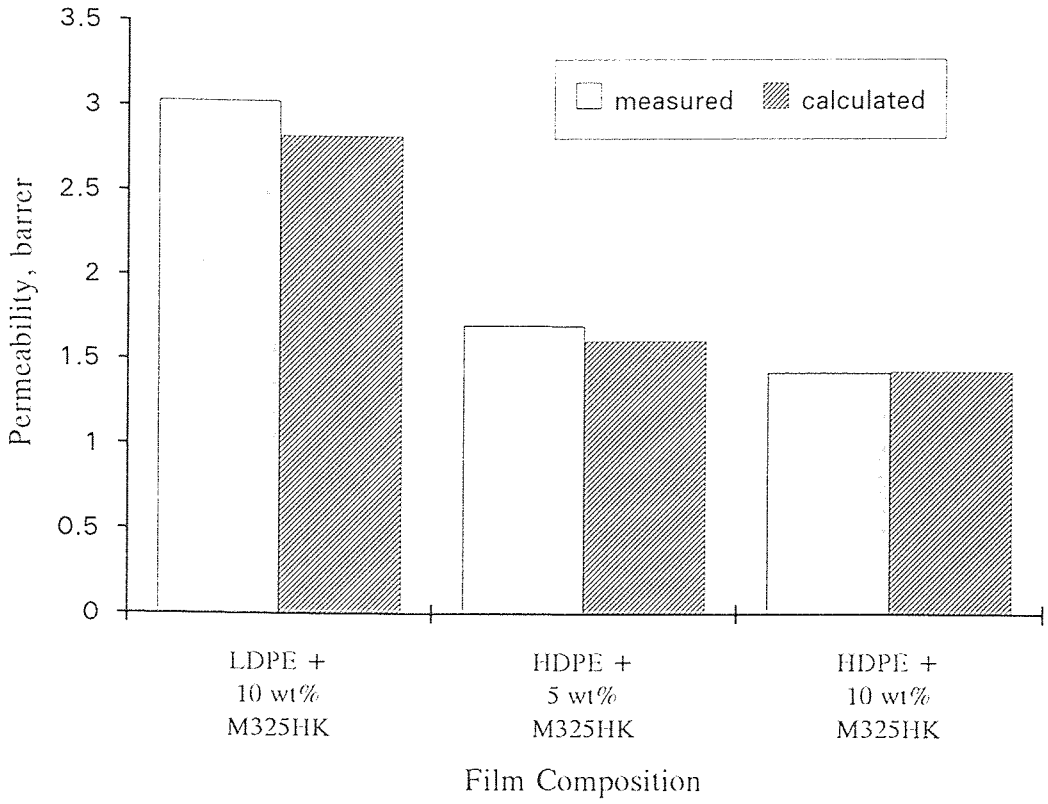

Figure 4.18 Comparison of measured and calculated oxygen permeability for the polyethylene/mica films

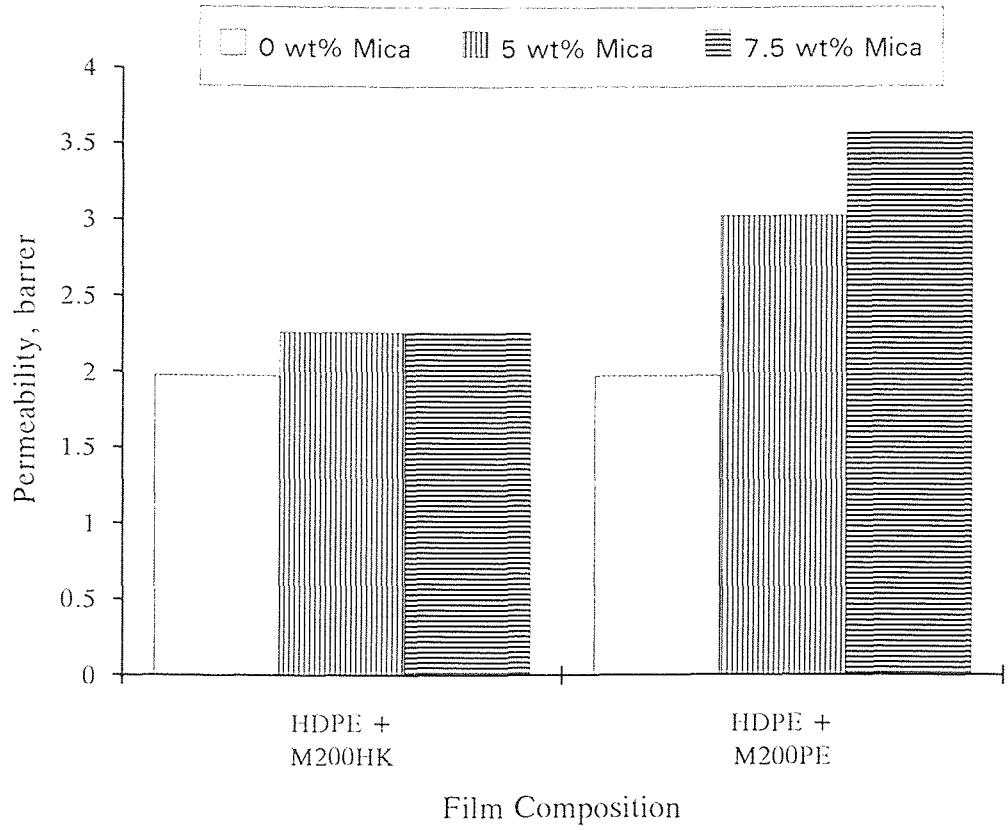

Figure 4.19 Effect of Mica200HK and Mica200PE on the oxygen permeability of HDPE films

CHAPTER 5

CONCLUSIONS AND RECOMMENDATIONS

The processability of PE/mica composites on the blown film extrusion line decreases with increasing the weight percentage of mica. This can be observed through the reduction of blow-up ratio and haul-off speed, and the increase of film thickness. HDPE with 10 wt% of mica is difficult to process since its films involved frequent bubble ruptures, so does the composite of HDPE/LDPE blends with 10 wt% of mica; however, LDPE with the same mica loading has no problem to process. Tension-thinning plays a major role in blown film extrusion, especially for HDPE and its mica composites.

The apparent shear viscosity of polyethylenes increases with increasing mica concentration. At low shear rate, Mica325HK is the most effective in increasing the viscosity among the three types of micas. At shear rates greater than 500 s^{-1}, only the composites with higher mica loadings show significant increases in viscosity. Increases in viscosity may have an adverse effect on processability. The results of the melt elasticity index measurements, however, appear to be somewhat in disorder without providing a correlation between melt elasticity and processability.

The mica flakes are well oriented with the broad faces parallel to the surfaces of blown films, and form overlapping discontinuous layers. The Mica325HK has a higher aspect ratio and finer particle size than the other two micas. With an increase of weight fraction of mica and a decrease of aspect ratio, the distance between the nearest neighboring layers decreases.

For blown films of polyethylene with all three types of mica, the tensile stress at yield and at break show a decline with increasing concentration, then tend to rise at both machine and transverse directions. For HDPE and its mica composites, the ultimate tensile stress is higher in the transverse direction, and so is the yield strength. Almost all the films have higher yield stress than stress at break. The elastic moduli of films in both directions increase with increasing mica concentration. On the other hand, the elongation at break of the films decreases dramatically with increasing mica loading, especially for HDPE/mica composites.

The oxygen permeability of unfilled polyethylene decreases with increasing density. The addition of Mica325HK can further reduce the oxygen permeability of polyethylenes because of the tortuosity effect. The other two types of mica used in this research showed opposite trends which could be attributed to a more random orientation and coarser particle size. We can conclude that the morphology of the polyethylene film is one of the most important factors particularly as related to changes in permeability.

In terms of recommendations, seeking optimum processing conditions is probably the priority, not only for making films at the higher possible filler loadings, but also for making films with microstructure more suitable to reduce permeability; meanwhile, study of the relationships between processability of blown film and melt elasticity/extensional viscosity should be of importance. The effect of interfacial agents (200PE vs. 200HK) on the morphology and properties of blown films was not demonstrated in this research and needs to be studied further. Finally, the comparison of the permeability values measured by different test methods, such as manometric determination, volumetric determination, and coulometric sensor, should be conducted for the same material when possible.

REFERENCES

1. M. M. Fox, *Physics and Chemistry of the Organic Solid State,* Vol. II, Interscience, New York, 1965.

2. J. Comyn, *Polymer Permeability*, Elsevier Applied Science Publishers, London, 1985.

3. D. W. Van Krevelen, *Properties of Polymers*, 3rd Ed., Elsevier, New York, 1990.

4. R. M. Felder and G. S. Huvard, *Methods of Experimental Physics*, Academic Press, New York, 1980.

5. "Standard Test Method for Determining Gas Permeability Characteristics of Plastic Film and Sheeting", ASTM D 1434-82, (Reapproved 1992).

6. "Standard Test Method for Oxygen Gas Transmission Rate Through Plastic Film and Sheeting Using a Coulometric Sensor", ASTM D 3985-81, (Reapproved 1988).

7. W. R. Vieth, *Diffusion in and through Polymers*, Oxford University Press, New York, 1991.

8. C. J. Heffelfinger, "A Survey of Film Processing Illustrated With Poly(Ethylene Terephthalate)", *Polym. Eng. Sci.*, **18**, 1163 (1978).

9. S. W. Lasoski, Jr., "Moisture Permeability of Polymers - Effect of Symmetry of Polymer Structure", *J. Appl. Polym. Sci,* **4**, 118(1960).

10. J. Perdikoulias and W. Wybenga, "Designing Barrier Film Structures", *Tappi Journal*, **72**, 107 (1989).

11. L. A. Kleintjens and P. J. Lemstra, *Intergration of Fundamental Polymer Science and Technology*, Elsevier, London, 1985.

12. M. A. Barger, W. J. Schrenk, D. F. Pawlowski, and J. N. Bremmer, "Lamellar Injection Molding", *Injection Molding*, **37**, 1, 1994.

13. P. G. Mercer, "Measurement and Control of Barrier Layers", *Tappi Journal*, **73**, 195 (1990).

14. S. R. Tanny, "Optimizing the Performance of Coextrudable Adhesive Resins", *Tappi Journal*, **74**, 109 (1991).

15. Donald. V. Rosato and Dominick V. Rosato, *Plastics Processing Data Handbook*, Van Nostrand Reinhold, New York, 1990.

16. P. Mapleston, "Barrier Film Coatings Add Performance Options", *Modern Plastics*, **69**, 48 (1992).

17. L. E. Nielsen, "Models For the Permeability of Filled Polymer Systems", *J. Macromol. Sci.*, **A1**, 929(1967).

18. T. M. Yeh, C. Y. Chen, S. J. Liour, and C. S. Tuan, "Effective Diffusivity Based on Morphology of HDPE/NYLON Composite", *ANTEC'95*, 1542 (1995).

19. G. W. Lohfink and M. R. Kamal, "Morphology and Permeability in Extruded Polypropylene/Ethylene Vinyl-Alcohol Copolymer Blends", *Polym. Eng. Sci.*, **33**, 1404 (1993).

20. M. R. Kamal, H. Garmabi, S. Hozhabr, and L. Arghyris, "The Development of Laminar Morphology During Extrusion of Polymer Blends", *Polym. Eng. Sci.*, **35**, 41 (1995).

21. H. Garmabi, M. R. Kamal, "The Development of Laminar Morphology in Extruded Polyethylene/Polyamide Blends", *ANTEC'95*, 3182 (1995).

22. K. Miura, E. Mori, K. Yoshizumi, A. Hiraku, and T. Goto, "Manufacturing Technology of Plastic Fuel Tank with High Fuel Permeation Resistance", *TOYOTA Technical Review*, **44**, 113 (1994).

23. N. G. McCrum, C. P. Backley, and C. B. Bucknall, *Principles of Polymer Engineering*, Oxford University Press, New York, 1988.

24. P. M. Subramanian, "Polymer Blends: Morphology and Solvent Permeability", *Proc. ACS, Polymer Prepri*nts, p.28 (April, 1989).

25. P. M. Subramanian and V. Mehra,"Laminar Morphology in Polymer Blends: Structure and Properties", *Polym. Eng. Sci.*, **27**, 663 (1987).

26. M. Xanthos, J. Grenci, and S. S. Dagli, "Polyolefin Blends with Low Oxygen Permeability", *SPE ANTEC*, **2**, 3194 (1995).

27. N. S. Murthy, A. M. Kotliar, J. P. Sibilia, and W. Sacks, "Structure and Properties of Talc-Filled Polyethylene and Nylon 6 Films", *J. of Appl. Polym. Sci.*, **31**, 2569 (1986).

28. J. Keating, "The Use of Barium, Calcium and Talc in Plastics", *Polymer Modifiers and Additives conference, RETEC*, New Brunswick, NJ, October, 1994.

29. T. C. Bissot, "Effect of Platelet Orientation on Performance of High Barrier Resins with Platelet-type Fillers", *Proc. ACS, Polymer Preprints*, p.26 (April, 1989).

30. T. S. Gill and M. Xanthos, "Effects of Fillers on Permeability and Mechanical Properties of HDPE Blown Films", *Proc. 54th SPE ANTEC*, **42**, 1757 (1996).

31. H. S. Katz and J. V. Milewski, *Handbook of Fillers and Reinforcements for Plastics*, Van Nostrand Reinhold Company, New York, 1978.

32. L. R. Johnson, "Principle Properties", *Plastic Digest*, Edition 17, Vol. 2, D.A.T.A. Business Publishing, Englewood, CO, 1996.

33. C. D. Han, *Multiphase Flow in Polymer Processing*, Academic Press, New York, 1981.

34. A. Ponnusamy, Master of Engineering Thesis, Stevens Institute of Technology, Hoboken, NJ, 1996.

35. B. Maxwell, "The Melt Elasticity Index: A Quality Control Measure", *Plastic Eng.*, **43**, 41 (1987).

36. F. A. Ruiz and A. O. Bankole, "Mineral Reinforcement of Linear-Low Density PE Film", *SPE ANTEC*, **1**, 1670 (1992).

37. D. M. Simpson and I. R. Harrison, "The Effect of Processing Parameters on the Morphologies and Mechanical Properties of PE Blown Films", *SPE ANTEC*, Vol. 1, 1206 (1993).

38. M. Arina, A. Honkanen, and V. Tammela, "Mineral Fillers in Low Density Polyethylene Films", *Polym. Eng. Sci.*, **19**, 30 (1979).